Numerical Study of the Effect of Turbulent Wake of Cylinder on Vortex Shedding from Flat Plate in Tandem Arrangement

Dariush Firouzbakht

Submitted to the
Institute of graduate studies and research
in partial fulfillment of the requirement for the degree of

Master of Science
in
Mechanical Engineering

Eastern Mediterranean University
June 2014
Gazimağusa, North Cyprus

Approval of the Institute of Graduate Studies and Research

Prof. Dr. Elvan Yılmaz
Director

I certify that this thesis satisfies the requirements as a thesis for the degree of Master of Science in Mechanical Engineering.

Prof. Dr. Uğur Atikol
Chair, Department of Mechanical Engineering

We certify that we have read this thesis and that in our opinion it is fully adequate in scope and quality as a thesis for the degree of Master of Science in Mechanical Engineering.

Assoc. Prof. Dr.Hasan Hacışevki
Supervisor

Examining Committee

1. Prof. Dr. Hikmet Ş. Aybar _____
2. Prof. Dr. Fuat Egelioğlu _____
3. Assoc. Prof. Dr. Hasan Hacışevki _____

ABSTRACT

Disturbed regions of flow will always appear in presence of any fluid flow over a stationary or moving body. These regions structures depend on both flow characteristics as well as the body. Body shape, surface roughness, orientation, size, flow velocity and viscosity are all influential parameters in the extent of disturb region. The flow structure behind multiple arrangements on bluff bodies are still an interesting subject and vastly under research because of the interaction between wakes. The development of different computational fluid dynamics (CFD) codes and commercial software are all as a result of this need for better understanding on the flow behavior.

Vortex shedding from different bluff geometries is one of the most attractive and significantly important areas in fluid mechanics. Recent years with global warming issues caused by aerodynamic drag forces, rising fuel prices and safety measures, the vortex shedding has become more important. Energy conservation examples include but not limited to automobiles and skyscrapers (convection heat loss). Furthermore, it is important in structural design to limit the oscillation amplitude of the structure as well as preventing resonance phenomena.

Simulation the flow structure and characteristic behind a circular cylinder and a normal flat plate in tandem arrangement with the same diameter and width at six gap ratios was performed. The impact of the circular cylinder turbulent wake on shedding frequency and Strouhal number of the plate were the main aim of this study.

Commercial computational fluid dynamics software, ANSYS/CFX 15.0® was used. Shear stress transport turbulent model were used as simulation technique.

The geometry modeling was done with respect to the test section of the EMU Mechanical Engineering Aerodynamics laboratory for data comparison in future studies and justification of the results. The shedding frequency and Strouhal number for each case were calculated and compared with respect to geometry and gap ratio.

Keywords: Vortex Shedding, Bluff Bodies, Strouhal Number, Shedding Frequency

ÖZ

Sabit veya hareketli cisimlerin etrafindaki uyarılmış akışkan akımı her zaman gözlemlenmektedir. Bu bölgesel yapılar akış karakteristiklerine ve cisimlerin şekline bağlıdır. Cismin şekli, yüzey pürüzlülüğü, oryantasyonu, boyutu, akış hızı ve viskozitesi uyarılmış bölge içinde etkili olan parametrelerdir. Değişik düzenlemelerdeki yapıların arkasındaki akış yapılarının oluşturduğu dalgalar arasındaki etkileşim hala daha ilgi çekici olmakta ve çeşitli araştırmalara konu olmaktadır. Geliştirilmiş olan birçok CFD (Bilgisayar Destekli Akışkanlar Mekaniği) kodu ve programı akış davranışlarını anlamak için geliştirilmişitr.

Değişik geometrilerin Vortex oluşumu akışkanlar mekaniğinin en çekici ve önemli alanlarından biridir. Son yıllarda küresel ısınma, yakıt fiyatlarındaki artış ve güvenlik ölçütleri ile girdap oluşumları daha önemli hale gelmiştir. Enerji tasarrufu örnekleri, sadece otomobille sınırlı değil gökdelenleri de kapsamaktadır (konveksiyon ısı kaybı). Ayrıca, yapısal tasarımlarda yapının salınım amplitüdünü limitlemek yanında rezonans olgularını sınırlamak da önemlidir.

Bu çalışmanın amacı, altı değişik boşluk oranında aynı çapa ve genişliğe sahip arka arkaya dizilmiş bir silindir ve normal bir düz plaka arkasında akım yapısını ve özelliklerini canlandırmaktır. Bu çalışmanın esas amacı dairesel silindirin turbulent dalgasının, düz plakanın sarmal frekansı ve Strouhal sayısının üzerindeki etkisini araştırmaktır. Çalışmada ticari olarak hazırlanmış hesaplamalı akışkanlar dinamiği yazılımı , ANSYS / CFX 15.0 ® kullanılmıştır.

Kesme gerilmeli taşıma turbulans modeli simülasyon tekniği olarak kullanılmıştır. Geometrik modelleme gelecekteki çalışmaları ve sonuçları mukayese edebilmek için DAÜ Makine Mühendisliği Aerodinamik laboratuvarındaki rüzgar tüneli test bölümüne göre yapılmışır. Her bir geometri ve boşluk oranı için sarmal frekansı ve Strouhal sayısı hesaplanıp karşılaştırılmıştır.

Anahtar Kelimeler: Vortex oluşumu, Hesaplamalı Akışkanlar Dinamiği, Kaba gövde, Strouhal Number, Shedding Frequency

ACKNOWLEDGMENT

My special thanks to my supervisor Assoc. Prof. Dr. Hasan Hacişevki for his help and understanding and the influence of his guidance on my work. Also, I would like to thank my family, Hamid, Zohreh and Koorosh for their continuous support, love and encouragement.

TABLE OF CONTENTS

LIST OF TABLES

LIST OF FIGURES

NOMENCLATURE

C_l	*Two* Dimensional Lift Coefficient
C_d	*T*wo Dimensional Drag Coefficient
d	Circular Cylinder Diameter [mm]
f	frequency
g	Center to Center Gap [mm]
g/w	Gap ratio
Re	Reynolds Number, $Re = \rho u d/\mu$
St	Strouhal Number, $St = fd/u$
S_{Mx}	Total body forces in X direction per unit area [N/m^2]
S_{My}	Total body forces in Y direction per unit area [N/m^2]
S_{Mz}	Total body forces in Z direction per unit area [N/m^2]
T	Temperature [K]
u	X Direction Velocity Component [m/s]
u'^2	Normal Reynolds Stress in *x*- direction [m^2/s^2]
v	Y Direction Velocity Component [m/s]
w	Z Direction Velocity Component [m/s]
W	Plate Width [mm]
w'^2	Normal Reynolds Stress in *z*- direction [m^2/s^2]

Greek Symbols

β	Thermal Expansion Coefficient [1/K]
λ	Second coefficient of viscosity [kg/m.s]
μ	Dynamic Viscosity [kg/m.s]
ρ	Density [kg/m^3]

ϕ Dissipation function

Abbreviations

CFD Computational Fluid Dynamics

FFT Fast Furrier Transform

LIF Laser Induced Fluorescence

SST Shear Stress Transport Turbulence Model

Chapter 1

INTRODUCTION

1.1 Computational Fluid Dynamics

Fluid behavior in interaction with solids or other fluids has been studied and analyzed vastly by scientists and engineers for centuries now. The first major study of this field goes to ancient Greece. Archimedes' principle may be the first published study on fluid behavior. Later, Leonardo da Vinci, Evangelista Torricelli, Isaac Newton, Blaise Pascal, Daniel Bernoulli, Claude-Louis Navier, George Gabriel Stokes and others have all contributed to this field. There are two major approach in fluid dynamics, one being experimental and the other theoretical or numerical. Experiments and wind tunnels are used to study the fluid behavior. The wind tunnel testing is a powerful simulation tool and very helpful during design stages but the cost of running wind tunnel testing is very high, the equipment are expensive and it is very time consuming. Furthermore, there is a scaling issue for large bodies like aerial vehicles, ships and submarines. These factors and mathematical progress together with the advent of computers enabled the engineers to come to a cheaper solution called computational fluid dynamic or in short CFD. In other words, analysis of fluid flow, heat transfer and associated phenomena through Computer simulation [1]. The application of this technique is widely associated with the advent of high speed computers.

The mathematical statement of governing equations of moving fluid is the conservation law of physics which are conservation of mass, momentum (Newton's second law) and energy (Thermodynamics first law). In every point of the domain all three for mentioned laws must be satisfied. Numerical solution to these expressions is the sole purpose of CFD.

1.2 Problem Statement

The aim of this thesis is to numerically analyze the unsteady wake structure and flow parameters including Strouhal number behind a circular cylinder and flat plate in a row at different gap ratio with the same diameter and width as well as length ratio of 0.5. The effect of circular cylinder wake on shedding from normal flat plate was investigated with regard to gap ratio and geometry. The Reynolds number set to the magnitude of 33,000 so the unsteady turbulent wake occurs. Another reason for selecting this number was that the equipment needed for experimental verification of the output data was available at the Eastern Mediterranean University (EMU) Aerodynamics laboratory so future studies can be done on this case. Furthermore, two tandem flat plates also simulated for the code verification.

The model used was the exact replica of the wind tunnel test section of the EMU Aerodynamics laboratory. The model was created using SOLIDWORKS software and then imported to the ANSYS/CFX 15.0®. The boundary conditions, input, output and wall are set to be exactly like the wind tunnel conditions. The ANSYS CFD Post was implemented for post processing the output data. Additional expressions were added to the CFX setup to obtain Strouhal Number (St), lift coefficient (C_l) as well as the drag coefficient (C_d). Furthermore, shedding frequency and St number were also obtain by performing Fast Furrier Transform (FFT) on C_l.

FFT can be also perform on pressure or velocity at any points downstream of the unsteady wake which gave the same results as performing FFT on plates C_l. Appropriate turbulent models for this case was selected according to literature and previous studied on similar cases.

1.3 Practical Importance of Vortex Shedding in Engineering

Vortex shedding from different bluff geometries is one of the most attractive and significantly important areas in fluid mechanics. Recent years with global warming issues, raising fuel prices and safety measures, the vortex shedding has become more important. Energy conservation examples include but not limited to automobiles, skyscrapers (convection heat loss) and heat exchangers. Furthermore, it is important in structural design to limit the oscillation amplitude of the structure as well as preventing resonance phenomena. This occurs when the shedding frequency is close or higher than the natural frequency of the structure. The famous failure of Tacoma Narrows Bridge in 1940 is a subject of a chapter of nearly every Physics book. The resonance induced by wind caused the collapse of the bridge.

1.4 Processing the Problem Using CFD

Every CFD code consists of three distinguished main steps: Pre-Processor, Solver and Post-Processor. The first step is to import the flow problem in to CFD software or code in a form which is suitable for the solver. The solver used numerical techniques to reach a solution. And finally Post-Processor which as it name would suggest enable the user to analyses the data generated by the solver.

For the current study the following steps were taken to reach the output data for CFD Post-Processor:

- The geometries were generated using SOLIDWORKS

- Unstructured mesh was generated by CFX commercial mesh software
- Flow properties were define
- Unsteady flow were selected because of the nature of the shedding phenomena
- Appropriate time step was selected
- Suitable turbulence model was selected
- Boundary conditions were defined
- Initial conditions were defined
- Additional expressions were define for the software to be used in Post-Processor
- Solver was initiated

1.5 Discussion of the Following Chapters

Both experimental and numerical studies previously done on the unsteady shedding case is presented in chapter 2. Chapter 3 contains the methodology used for solving the problem and the reasoning for choosing to do so, followed by the solver output and results. Graphs and contours are implemented for better illustration of the generated data. Finally chapter 5 consists of conclusion of this thesis and the future work which can be done.

Chapter 2

LITERATURE REVIEW

Significance of the wake of bluff bodies and specially vortex shedding phenomena was well illustrated in chapter one. The purpose of this chapter is to try a thorough literature review of the previous work done regarding the problem at hand. Both experimental and computational i.e. theoretical approaches will be presented.

2.1 Experimental Approaches

Using hot wire anemometer, for a two dimensional bluff body for Reynolds number range 1.4×10^5 to 2.56×10^5, P.W.Bearman [2] measured the base pressure, shedding frequency and traverse of the wake. The body had blunt trailing edge. At single base height from the back face of the body, traverses illustrated a peak in the RMS velocity fluctuation which was fully formed vortex. Furthermore, continuing with splitter plates up to four height of the base added to model, the position of the fully formed vortex was found and a inverse proportion between distance from model and base pressure coefficient was discovered. Adding splitter plates to the model reduced the drag coefficient and in some tests suppresses the formation of the vortex.

Auteri F. et. al. [3] investigated the flow structure behind two normal flat plates using wire anemometer signal for Re=8340 for gap ratios of 0.25 to 7.5. They reported the relationship between St Number and the gap ratio. They found the presence of two different flow regions, depending on the gap ratio and at gap ratio around 0.9 both

regions appear alternatively. Furthermore, oil smoke was used to further investigate the mechanism of shedding regions. [3]

The experiment on tandem arrangement square cylinder was carried out by Chi Hung Liu and Jerry M.Chen [4]. They investigate the influence of gap ratio and also the manner of changing the spacing ratio on flow parameters. Using low speed open type wind tunnel, the spacing of the models were changed in the way of progressive increase as well as progressive decrease ranging from 1.5 to 9.0 times the width of cylinder. Reynolds number were also were changed ranging 2.0×10^3 to 1.6×10^4. For all the range of Reynolds numbers which was simulated in tunnel the occurring hysteresis was corresponded to two different flow pattern: mode I and II. Also two distinguished jump were observed in hysteresis regime. The hysteresis was also observed in Strouhal number but only with a single distinguish jump at lower spacing limit of the regime. Corresponding to a different mode for higher Reynolds numbers the same shedding frequency could occur at the upper spacing limits. On the side and rear face of the upstream cylinder as well as front and side face of the downstream cylinder a massive decrease in fluctuating pressure were detected as Reynolds number reached 8000 and 16000 in mode II. This shows that for bigger Reynolds number the vortex shedding is weaker for the upstream cylinder. [4]

Experimental study for two tandem square cylinder with the same width using vertical water container was done by S. C. Yen et al. [5] so that the effect of Reynolds number, gap ratio and rotation angle of second cylinder on flow structure can be retrieved. By the use of particle image velocimetry(PIV) system and topological analysis flow patterns, turbulence parameters and force coefficient are

determined. Changing the gap ratio and Reynolds number lead to three distinguish category of flow fields: single mode, reattached mode and binary mode. Also, by changing the gap ratio and downstream cylinder incidence the flow can be categorized by six flow fields. The first mode which was the single mode is similar to a single cylinder. The reattached mode refers to the reattachment of the vortices and the binary mode represents the simultaneous shedding. The findings showed at low ranges of Reynolds numbers that the Strouhal number decrees as it increases. Although after reaching high Reynolds number, Strouhal increases and after a certain point it become somehow constant. [5]

Using two hot wires at the same time and Laser-induced fluorescence (LIF) visualization, G. Xu and Y. Zhou [6] calculated the Strouhal numbers and shedding frequency for two in inline cylinders. The Reynolds range was 800 to 4.2×10^4 with the gap ratio changing from 1 to 15.

They concluded that the Strouhal number exceptionally influenced by the gap ratio. For the gap ratios less than the critical gap ratio ($3.5< (L/D)_c<5$) no vortex street to be found in the gap and the Strouhal number drops in a fast manner for higher gap ratios. For gap ratios bigger than the critical ratio, the vortices shedding can be seen from both cylinder or in other words co shedding occurred with the equal frequencies and increasing the gap ratio would increase the value of Strouhal number to 0.18 and 0.22 for gap ratios higher than 10. Based on flow characteristic and behavior they categorized four different shedding modes:

1) For the gap ratios between 1 and 2 the separated flow from first cylinder were rolled behind the second cylinder.

2) For the gap ratios ranging from 2 to 3 there is a transition from rolled up flow in the wake of first cylinder to reattachment.

3) For the range 3 to 5, transition was from reattachment to co-shedding.

4) And finally for gap ratios higher than 5 only co shedding appeared.

They concluded that for the fourth mode the shedding frequencies are the same and Strouhal number raised up and reach a constant value with increase in gap ratio. For the first mode by increasing the gap ratio reduced the Strouhal number value as well as for the second and third modes. [6]

Another study on the wake characteristics of two different cross sectional bodies, side by side, has been done by Chin Yi Wei and Jeng Ren Chang [7] using a closed, low speed wind tunnel and aided by visualization with water table. Two dimensional plates, circular and square cylinders were adapted as test models. The tests were divided into two sets, bluff bodies with different geometries but the same shedding frequencies and bluff bodies with the same geometries but different shedding frequencies. The Reynolds number range of this study was 4000 to 6000. They found that the wake structure and base-bleed of the flow in strongly depend on the geometries. They concluded that for small gap ratios the downstream shedding frequency of the two bluff body arrangement is nearly half of the average shedding frequency in single bluff body case. For large gap ratios the wake acts as a single bluff body case as expected. As a result of analyzing the biasing behavior of the gap flow, they also found out the flow tended to deflect toward the downstream wake of two side by side bodies. Furthermore, the gap flow had somehow unstable biasing characteristic while wake width downstream of bodies were nearly equal.

M.Kiya and M.Matsumara [10] studied the fluctuation of frequency components of incoherent velocity in the downstream wake of a normal flat plate. The data were acquired downstream of the plate in the periodic wake at eight times of the plate heights. They used a open-return low speed wind tunnel with the test section of 0.30m×0.03m and the free stream velocity of 16.4(m/s). X-wire probes with constant temperature hot wire anemometers were used to measure the velocity fluctuations in the wake. The components of the incoherent fluctuations shear stress had frequencies around half of the shedding frequency.

Cetin Mazharoglu and Hasan Hacişevki [8] used open low speed wind tunnel to investigate the unsteady wake behind a single plate as well as two plates in tandem arrangement [9]. The study was done with constant flow velocity of 16.4±0.02 (m/s) and Reynolds number of 3.3×10^4. The plate width and thickness were selected in a way so the result could be comparable with the previous studies. Triple decomposition method together with phase averaging was used and the generated data were in agreement with M.Kiya and M.Matsumara's results by the factor of ±5% [10]. To maintain continuity, plate back face increased the width of the wake and decreased the velocities. Comparison of single flat plate case and double normal flat pates were done for several gap ratios. At the same position i.e. from the back face of single plate and from the back face of the second plate for double plate case, the velocity, coherent velocity and incoherent velocity contours were illustrated for the gap ratios of 0.5 and 1.0. The velocity contours that were obtained showed similar pattern with the exception of the peak value for single plate case being as much as 15% higher than double plate case. Also, for coherent velocity contours this phenomenon repeats itself but the peak value were reduced 12% from the single plate

to double plate with gap ratio 0.5 and increased for the gap ratio of 1.0. Furthermore, for the gap ratios of 0.5 and 1.0, the peak values of incoherent velocities of single plate were 70% and 40% higher than the double plate respectively.

Robert J. Martinuzzi and Brian Havel [11] used phase-averaged fiber optic Laser Doppler Velocimetry(LDV) to obtain shedding frequency and Strouhal number in wind tunnel for two tandem cubes with size H=0.04m and gap ratio of 2H for Re=22000 and 0.07H laminar boundary layer thickness . They used suction type wind tunnel with the test section of $0.46\times0.46m^2$, free stream velocity of 8.8 m/s and turbulence intensity less than 1.5%. For the gap ratios of 1.5 and 2.5the shedding frequency was scaled inversely with the gap and as a result the Strouhal numbers based on the gap were constant. In this regime the Strouhal number is geometrically locked and shedding is influence by the vertical and vortex in the gap interference. This three-dimensional phenomena was not observed in two-dimensional cases. They also showed that the structure of the turbulent field between two cubes was absolutely different from the base region of two-dimensional case. In two-dimensional shedding, the shedding was a result of interference between the forming vortex and the opposed shear layer but in three-dimensional case in the gap region, shedding was a result of interference of the normal stream of the front face of the second cube and the side shear layers. The coupling of the oppose vortex of the face of the second cube to the opposite shear layer result in stable periodic shedding. So they concluded that it is expected that the relationship between shedding frequency and the gap size is a linear one since the shedding is a result of vertical velocity stream and position of this stream depends on the location of the second cube. If the gap is big enough the shear layer would attach before the second cube and eliminate

the normal velocity stream and hence the locked region vanishes.

2.2 Computational/Theoretical Approaches

A. Sohankara et al. [6] simulate the flow around rectangular cylinders at different incidence for two dimensional, incompressible, unsteady condition with Reynolds numbers less than 200. The rectangle side ratio was between 1 to 4.The flow was assumed to be laminar. A SIMPLEC code and non- staggered grid were implemented. The results were compared to experimental data available. For convective terms a QUICK third order scheme were used. Implicit time discretization and second order Crank-Nicolson scheme were also used. They calculated the drag, lift, and moment coefficients as well as the Strouhal number. The results were depending on physical parameters such as Reynolds number, incidence angle and body side ratio. Furthermore, it was found that the results were depending on numerical parameters such as time step domain size and spatial resolution. With only one side opposing the flow with Re=100, the generated data showed that the separation occurred at downstream corners while at Re=200 it were from upstream corners. Separation at Re=200 is fully attached bubbles at projected ratio of $h/d \geq 2$. The change in reattached wake occurs in projected ratio in the range of 1.5 to 2. The behaviors of the flow parameters for incidence angle 20 to 70 degrees are not significantly different. On the other hand it is significant for $\alpha>70$ and $\alpha<20$ because of the flow evolution close to cylinder. [6]

Numerical simulation of the shedding flow passing over a square cylinder at the Reynolds number of 22,000 was done by Gerhard Bosch and Wolfgang Rodi [13]. The calculations were done at different adjacent wall positions with respect to the cylinder. Flow unsteady governing equations were solved numerically in two-

dimensional domain. Fluctuations due to turbulent were simulated with two k-ε turbulent model, standard k-ε turbulent model and the modified one by Kato and Launder [14]. They found out that the second model improved the generated results for vortex shedding significantly even with the adjacent wall presence. While the standard k-ε turbulent model suffered in smaller gap sizes as well as larger ones. The standard model did not illustrate the unsteady nature of the flow for smaller gap sizes and at larger gap sizes the shedding was damped too much. Meanwhile the Kato and Launder model removed the extreme turbulent kinetic energy production in stagnation areas which standard model predicted. Furthermore, with cylinder placed closer to adjusted wall, the results from both turbulent model became steady and the shedding vanished which is in agreement with the experimental results.

Two and three dimensional analysis of flow structure over two square cylinders in tandem arrangement with several gap ratios and Reynolds numbers were done by KatsuyaEdamoto and Mutsuto Kawahara [15]. The aerodynamics parameters were compared with the experimental results. The results of two dimensional analysis for the vortices behind the first cylinder over the wide range of Reynolds number were not in agreement with the wind tunnel tests for similar gap ratios and as a results the time averaged coefficients of pressure were not identical as well to experimental data except for the case of narrow or wide gaps. For the case of three dimensional analysis there were agreements between experimental and numerical data for Reynolds number range from 10^3 to 10^4 as well as the pressure coefficients for Reynolds number of 10^4.

Chapter 3

METHODOLOGY

3.1 Introduction

Numerical study were done to observed the effect of the cylinder turbulent wake on vortex shedding of the normal flat plate placed downstream of the circular cylinder in different gap ratios. Flow was considered to be two dimensional and the flow velocity were 16.4 (m/s) to achieve Reynolds number of 33,000. Finite volume method was implemented to solve the flow governing partial differential equations. The results were illustrated using contours and graphs for better understanding of the wake structure and flow characteristics. For simulation verification case of twin tandem plates turbulent shedding and laminar shedding from single cylinder were simulated as well. The plate dimension and geometry models were selected according to wind tunnel models and wind tunnel test section of the Aerodynamics laboratory of Eastern Mediterranean University. The tunnel test section is 0.5m*0.5m and length of 1.4metres. The plate width and cylinder diameter of the tunnel models are 30mm and their height is 0.5m. These dimensions give the blockage ratio of 6% which is small enough for reliable results from wind tunnel testing [21 and 22]. The geometries were generated by SOLIDWORKS commercial software and imported to the ANSYS CFX 15.0®. The simulation was carried out in four steps, meshing the geometries, setting up the problem, solver running and post processing the results. The fore mentioned steps are explained in detail in following sections.

3.2 Meshing

The geometries were imported to the CFX meshing from SOLIDWORKS. The streamwise axis was considered to be *x-axis* and the problem plane in two dimensional domain was *z-axis.* Both proximity and curvature functions were used to generate finest unstructured mesh possible. Ten layers of inflation with the growth rate of 1.2 were used in both cylinder and plate wall to better simulate the flow between two obstacles. Total number of elements in each simulation was around 400,000 and since the simulations were assume to be for two dimensional cases, the mesh were extrude once. The gap ratios were measured center to center i.e. from the cylinder center to plate center and change from 0.8 to 4. The mesh quality was checked with the program regularly for errors. After mesh was generated, the problem is ready to be defined for processing.

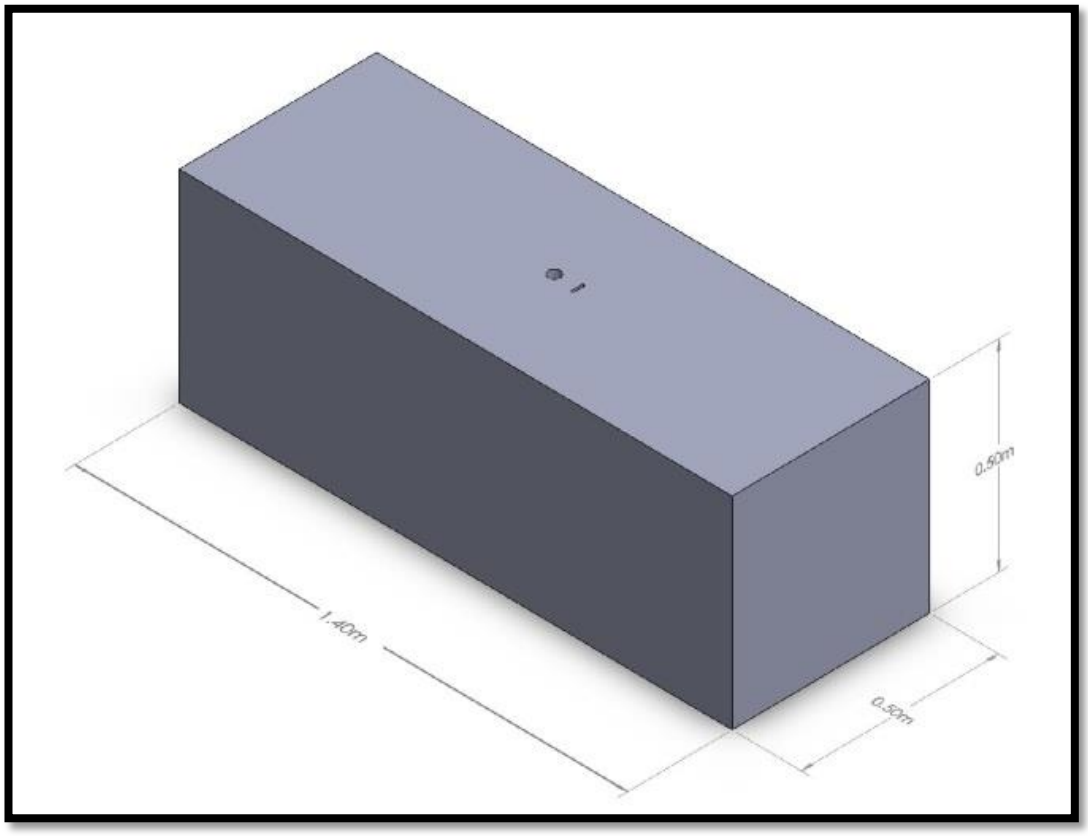

Figure 1. 3D Geometry Sample of EMU Wind Tunnel

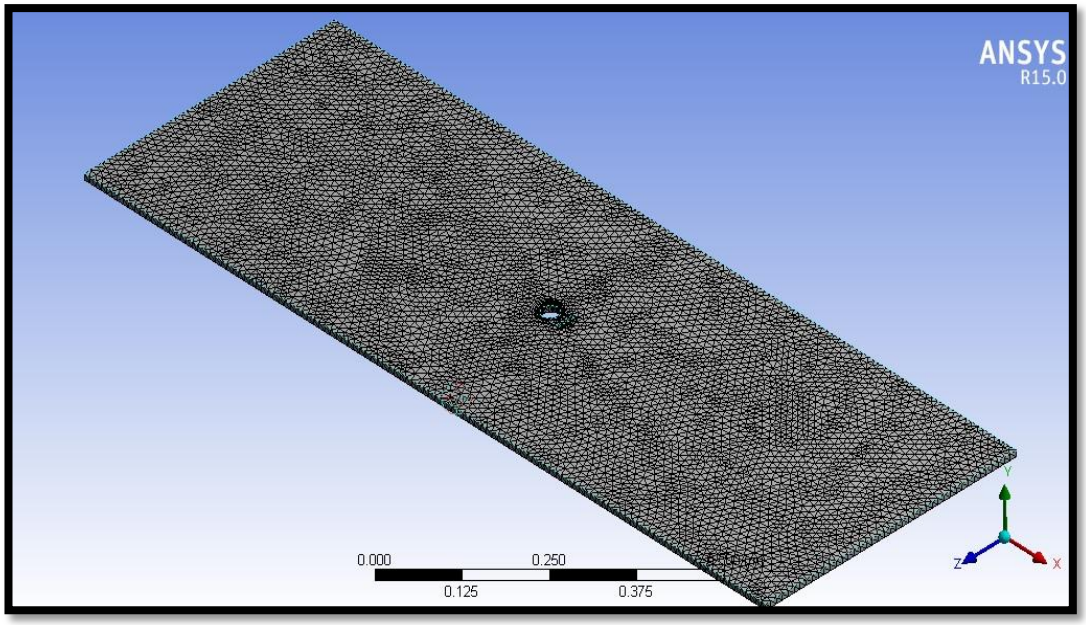

Figure 2. Sample 2D Meshing

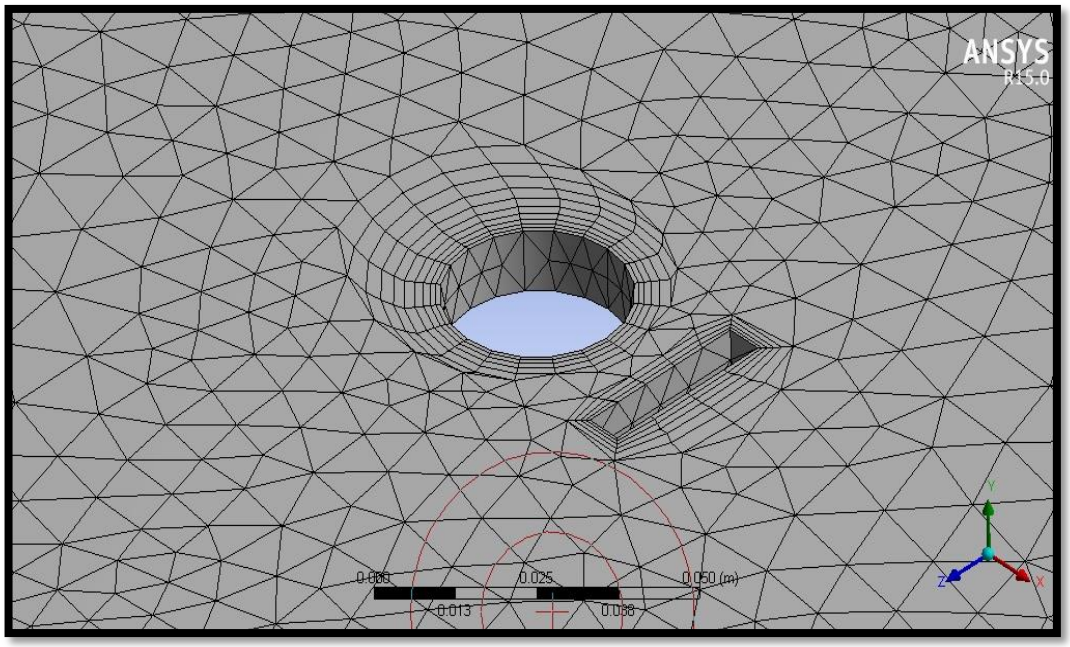

Figure 3. Sample Mesh Inflation Near wall and Gap

3.3 Problem Definition and Setup

3.3.1 Governing Equation

The flow governing equation must be solved and satisfied for each and every element in the domain [1]. These equations are as follow:

1) Conservation of mass which its interpretation is the rate of mass change within the element is equal to the mass removed from the element subtracted by mass added to the element:

$$\frac{\partial \rho}{\partial t} + \frac{\partial (\rho u)}{\partial x} + \frac{\partial (\rho v)}{\partial y} + \frac{\partial (\rho w)}{\partial z} = 0 \qquad \textbf{(3.1)}$$

Where, ρ is the fluid density and *u*, *v*, *w* are the velocity components in *x*, *y*, *z* direction.

2) The newton second law which is the rate of change in the momentum is equal to the sum of the force on the fluid element:

X momentum:

$$\frac{\partial (\rho u)}{\partial t} + div(\rho u \boldsymbol{u}) = -\frac{\partial P}{\partial x} + div(\mu\ gradu) + S_{Mx} \qquad \textbf{(3.2)}$$

Y momentum3.3equ

$$\frac{\partial (\rho v)}{\partial t} + div(\rho v \boldsymbol{u}) = -\frac{\partial P}{\partial y} + div(\mu\ gradv) + S_{My} \qquad \textbf{(3.3)}$$

Z momentum3.4equ

$$\frac{\partial (\rho w)}{\partial t} + div(\rho w \boldsymbol{u}) = -\frac{\partial P}{\partial z} + div(\mu\ gradw) + S_{Mz} \qquad \textbf{(3.4)}$$

Where P is pressure, μ is dynamic viscosity and S_{Mx}, $S_{My,}$ S_{Mz} are the total body forces on the element.

3) The rate of change in the energy is equal to sum of the heat addition to and the rate of work done on fluid element.

$$\rho c_p \left(u\frac{\partial T}{\partial x} + v\frac{\partial T}{\partial y} + w\frac{\partial T}{\partial z}\right) = \beta T \left(u\frac{\partial P}{\partial x} + v\frac{\partial P}{\partial y} + w\frac{\partial P}{\partial z}\right) + div(k\ divT) + \varphi \qquad \textbf{(3.5)}$$

Where c_p= specific heat

T = temperature

β =Thermal expansion coefficient

ϕ = Dissipation function with the following expression:

$$\phi = 2\mu(\frac{\partial u}{\partial x})^2 + 2\mu(\frac{\partial v}{\partial y})^2 + 2\mu(\frac{\partial w}{\partial z})^2 + \mu(\frac{\partial v}{\partial x} + \frac{\partial u}{\partial y})^2 + \mu(\frac{\partial w}{\partial y} + \frac{\partial v}{\partial z})^2 + \mu(\frac{\partial u}{\partial z} + \frac{\partial w}{\partial x})^2 + \lambda(\frac{\partial u}{\partial x} + \frac{\partial v}{\partial y} + \frac{\partial w}{\partial z})^2 \quad \textbf{(3.6)}$$

Where λ is the second coefficient of viscosity.

3.3.2 Heat Transfer and Compressibility Assumptions

Since the Mach number of the simulation was less than 0.3 the flow were treated as incompressible. Furthermore, since the simulation was done to determine the wake structure, the simulation was done isothermally and the energy equation was not solved numerically for time saving and since it didn't impact the generated results of the study.

3.3.3 Analysis Type and Time Step Selection

Since shedding is an unsteady phenomena, the problem was solved in transient mode with the time step of 0.0002s and total time of 0.2s for most cases and higher total run time for others to insure stable solution. The selection of the time step is very important to the result acquisition. The Strouhal number for a case of single plate at Reynolds number of 33000 is around 0.2. By assuming this number and calculation the shedding frequency, the shedding period were calculated and the selected time step is 1/50 of the shedding period. Second order backward Euler were used as transient scheme.

3.3.4 Boundary Conditions

Five types of boundary conditions were used as follow:

- Free slip Condition for tunnel walls
- No slip wall condition for plate and cylinder surfaces
- Inlet boundary condition set to the normal fluid velocity of 16.4(m/s), with the turbulent intensity of 0.08% and length scale of 0.0021m.

- Outlet boundary condition with relative pressure of 0 Pa.
- And finally the symmetry boundary condition in the extruded direction since the flow were simulated two dimensionally

3.3.5 Turbulence Model

Selecting a viscous model for simulation was the next step of setting up the problem. In general term, viscous models can be categorized by three general types, inviscid, laminar and turbulent viscous models. Selecting the model depends on the Reynolds number and for this study with the Reynolds number of 33,000 the viscous model was selected. The laminar shedding from the circular cylinder stats at Reynolds number 40 through 150 and for Reynolds number ranging 150 to 3×10^5 turbulent wake exists.

Turbulence nature of the wake was lead to select a turbulence model and since there is not a single global model for turbulent flow, the one appropriate for this case were chosen. The shear stress transport model (SST) was chosen for this study. This model is one of the most preferred models by the CFD users. Furthermore, because of the unsteadiness of the flow and the fact that this model shows goo result in both near wall and far from the wall, it was chosen. The SST turbulence model is very common model. It consists of two eddy viscosity equations. k-ω model is used for inner sections of boundary layer and it can be used through viscous sub layer and also it doesn't need any extra damping functions as well [19]. The shear stress transport model also switches to k-ε model in the free streams sections of the simulation and hence disposes of sensitivity of the k-ω model to turbulence properties. Also the SST has fare behavior in separated flows and negative pressure gradients [20].

The expressions for lift and drag coefficient added to the solver and monitored during the solver progress to both ensure the validity of the solution and also to be used in CFD post processing to calculate the Strouhal number.

3.4 Solver Run and CFD Post Processing

The solver was run for each gap ratio and results were saved for each time steps. The mass and momentum equation were solved for the every element of the domain and for each time step for the convergence of the solution 10 iteration were done and the root mean square (RMS) residual for momentum equation set to be 10^{-6}. CFD post processing were done with the aid of graphs and contours to better discover the nature of the flow. The results for each case are represented in the chapter 4 for same width and diameter plate and cylinder and for the half sized cylinder and full sized plate.

Chapter 4

RESULTS

This chapter represent the generated data in the CFD post processing of the of the wake structure of the twin inline circular cylinder and plate. The same problem was simulated by different gap ratios as follow:

$$\frac{g}{w} = 0.8, 0.867, 1.0, 2.0, 3.0 \; and \; 4.0$$

Where,

g = center to center distance

w = Plate Width

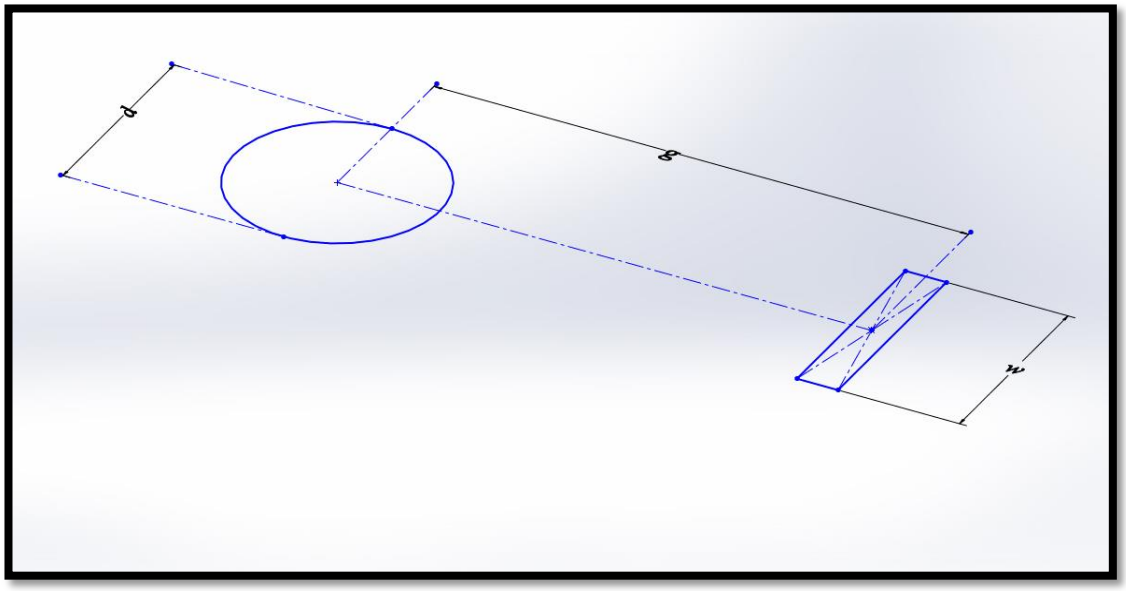

Figure 4. Geometry Parameters Definition

Furthermore, the same problem was simulated with the same geometries but different width to diameter ratios:

$$\frac{w}{d} = 1.0 \; and \; 2.0$$

Where,

d = circular cylinder diameter

The results for each case are presented in the following materials.

4.1 Plate and Circular Cylinder with Same Representation Length

Presenting all the ANSYS/CFX post CFD outputs are impossible and also there no point to do that as well. As samples several contours, graphs, vectors and stream line is presented for gap ratios of 2.0 and 4.0. For the gap ratios of 0.8, 0.867, 1.0 and 3.0 the calculated shedding frequency and Strouhal number are reported.

4.1.1 Gap Ratio of 4.0

The shedding frequency for the gap ratio of 4.0 was calculated to be 64.93Hz and the Strouhal number with the reference length of 0.03 (m) was 0.1188. The following contours were generated to illustrate the results better. The periodic lift coefficient chart is also presented as a sample.

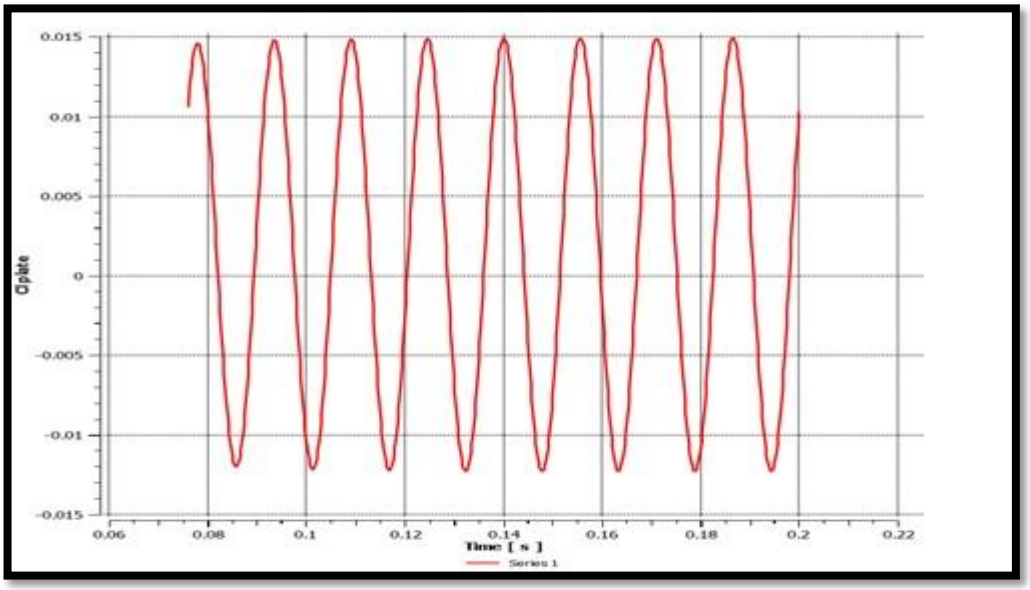

Figure 5. Periodic Lift Coefficient for $\frac{g}{w} = 4.0$

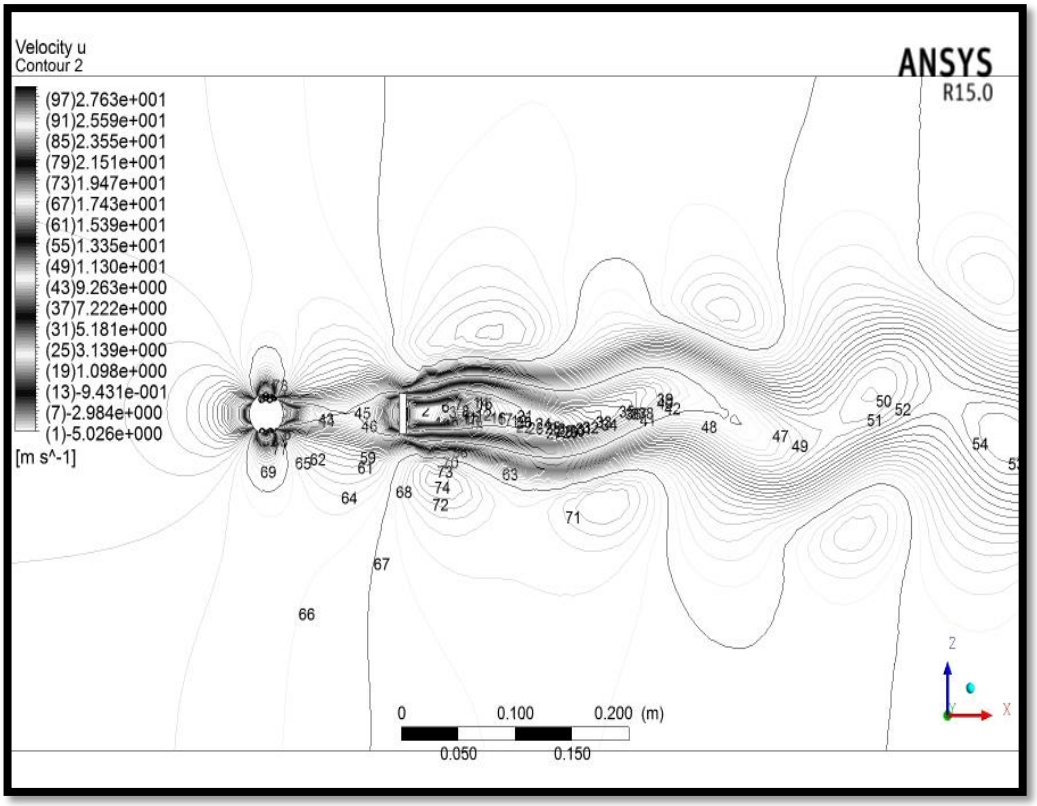

Figure 6. Contours of X-Velocity at t=0.200001s for $\frac{g}{w} = 4.0$

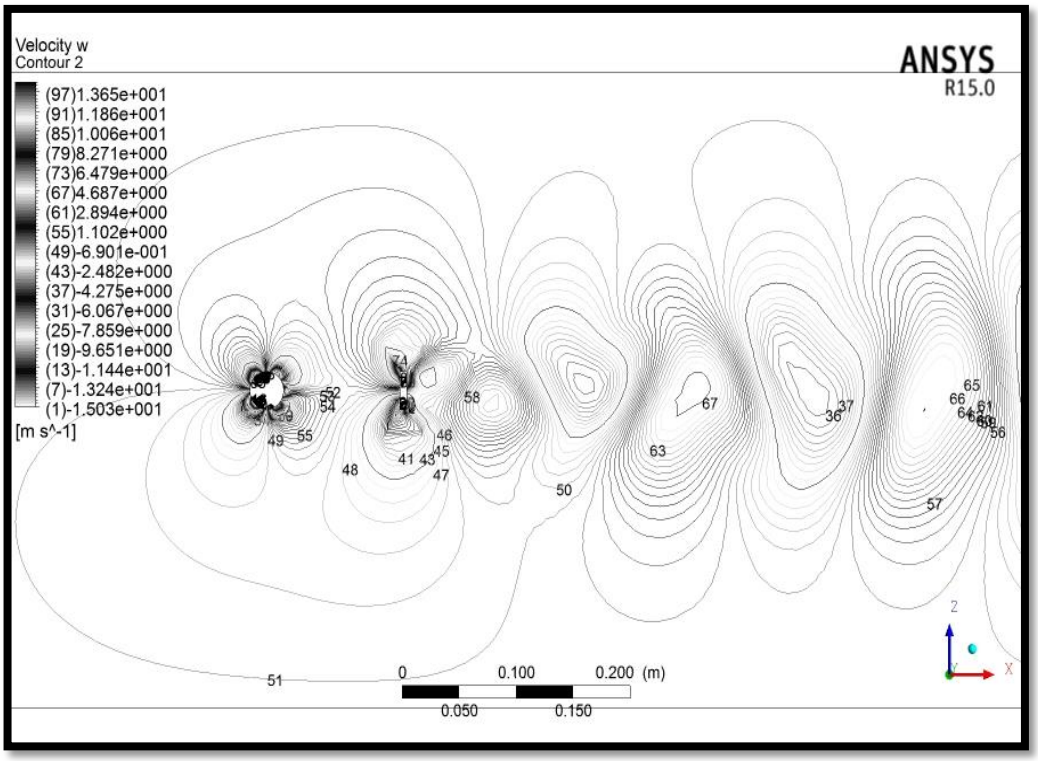

Figure 7. Contours of Z-Velocity at t=0.200001s for $\frac{g}{w} = 4.0$

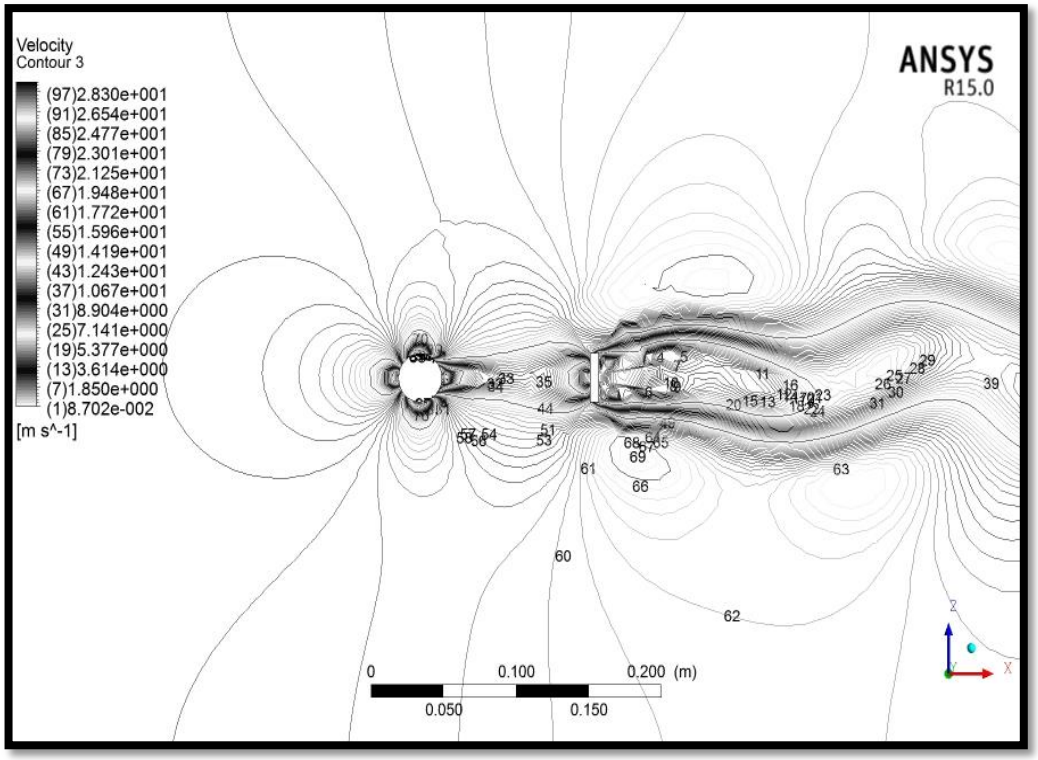

Figure 8. Contours of velocity at t=0.200001s for $\frac{g}{w} = 4.0$

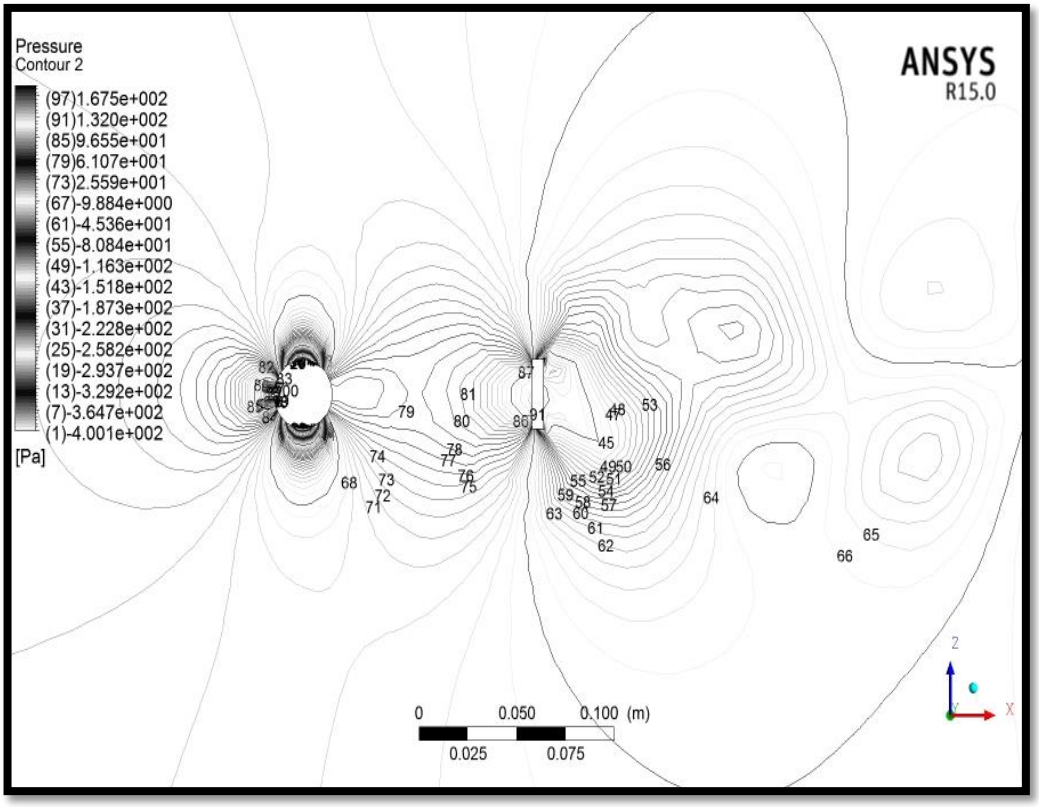

Figure 9. Contours of Pressure at t=0.200001s for $\frac{g}{w} = 4.0$

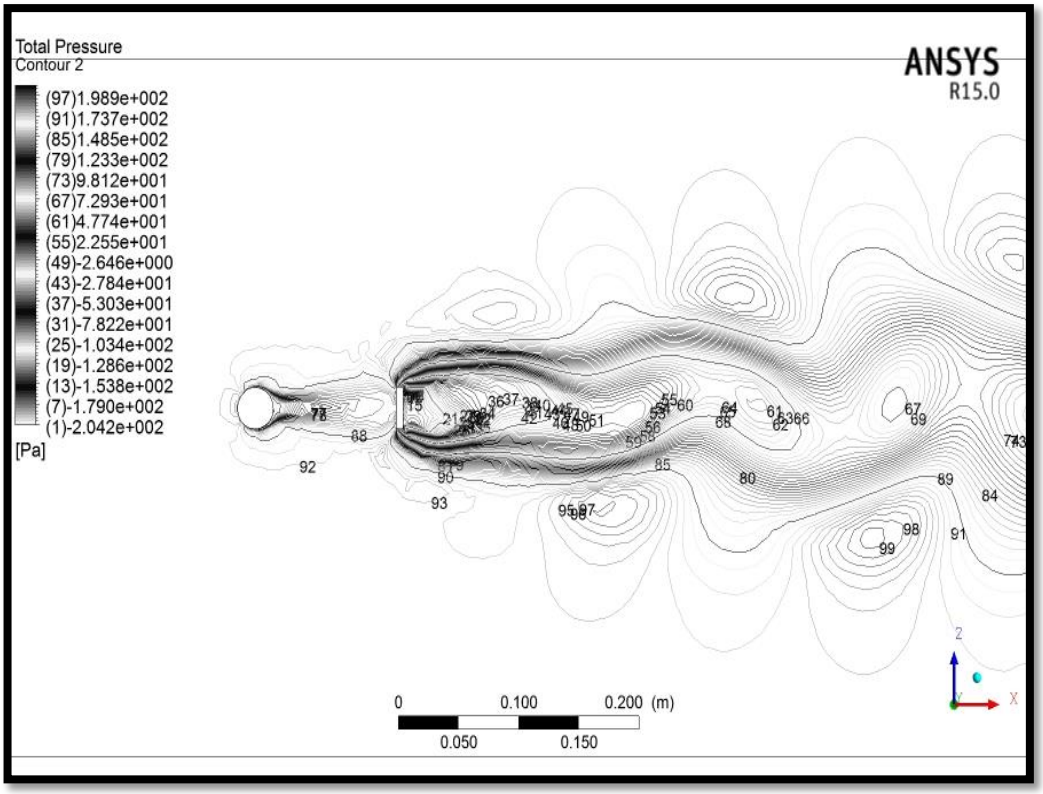

Figure 10. Contours of Total Pressure at t=0.200001s for $\frac{g}{w} = 4.0$

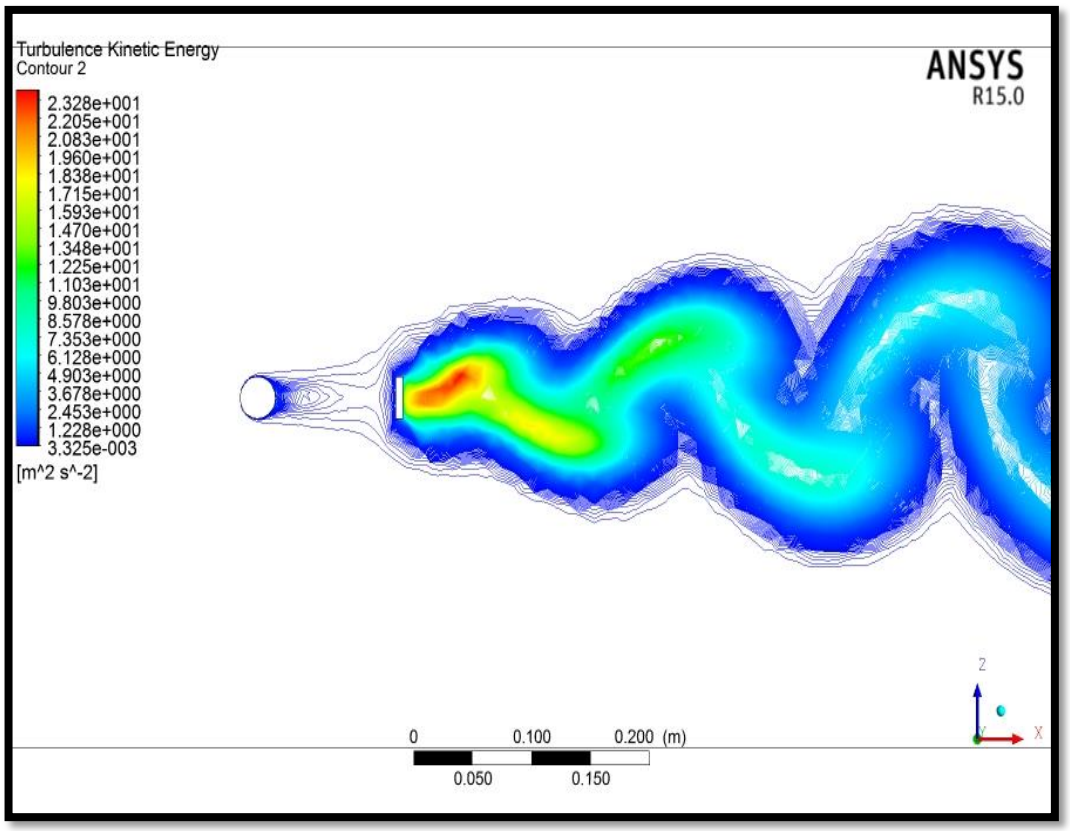

Figure 11. Contours of Turbulence Kinetic Energy at t=0.200001s for $\frac{g}{w} = 4.0$

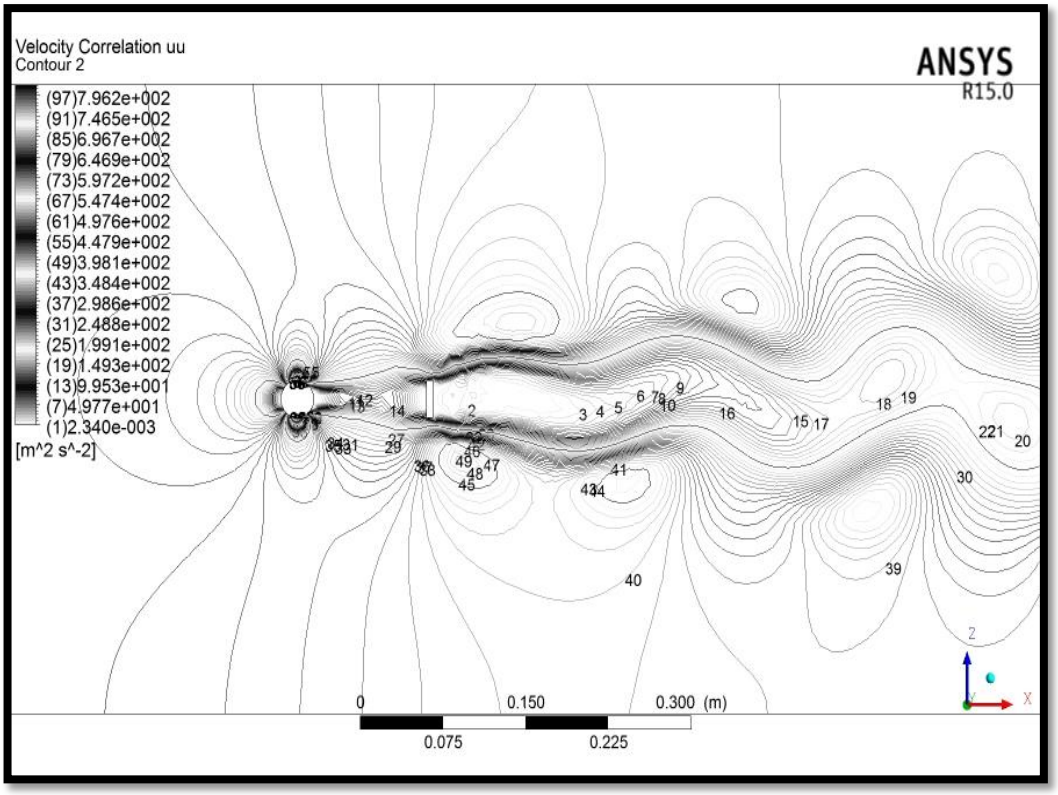

Figure 12. Contours of $u'u'$ Velocity at t=0.200001s for $\frac{g}{w} = 4.0$

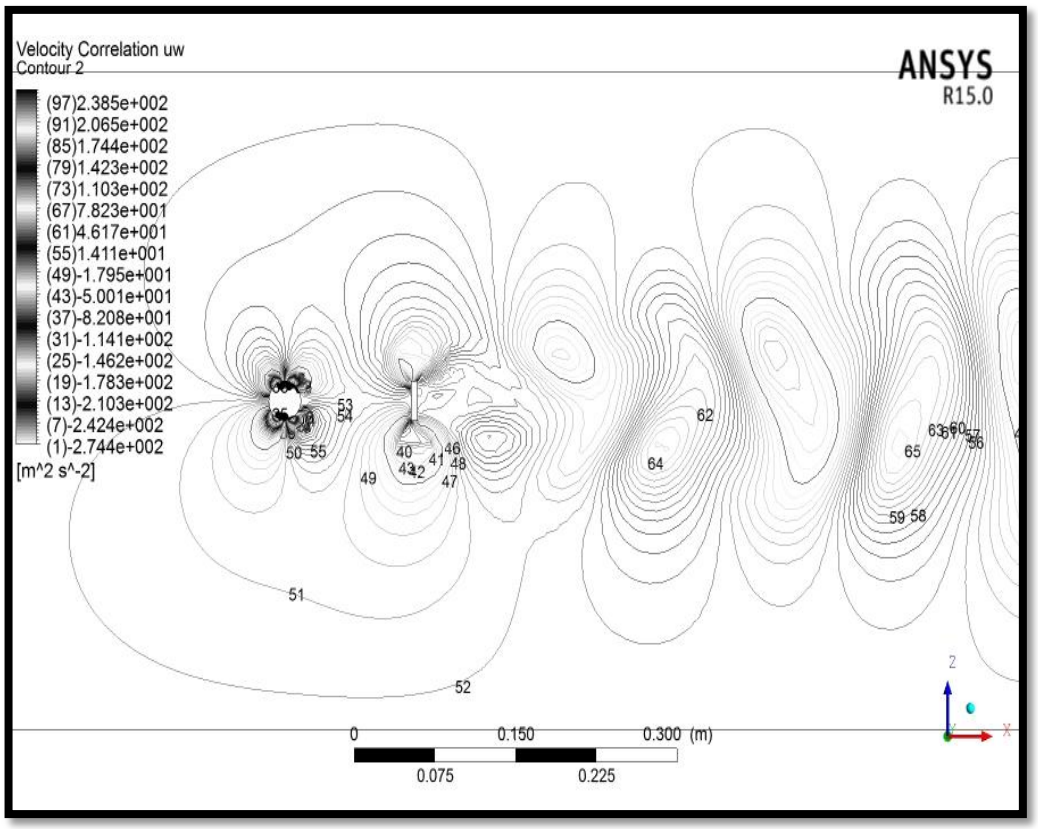

Figure 13. Contours of $u'w'$Velocity at t=0.200001s for $\frac{g}{w} = 4.0$

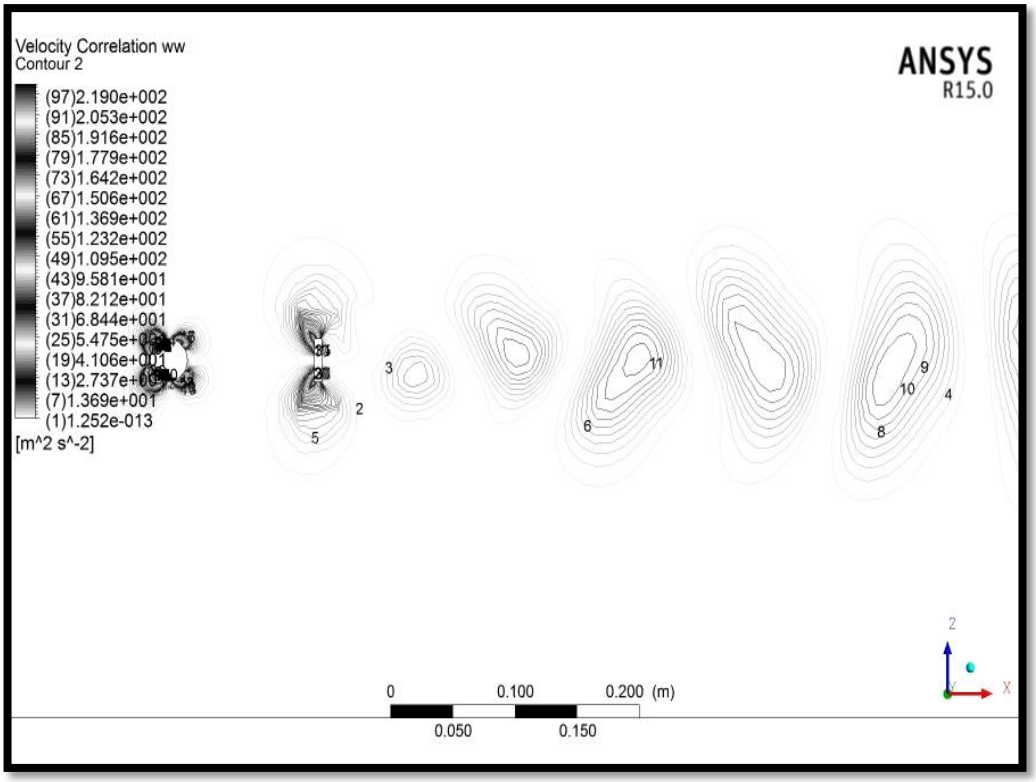

Figure 14. Contours of $w'w'$ Velocity at t=0.200001s for $\frac{g}{w} = 4.0$

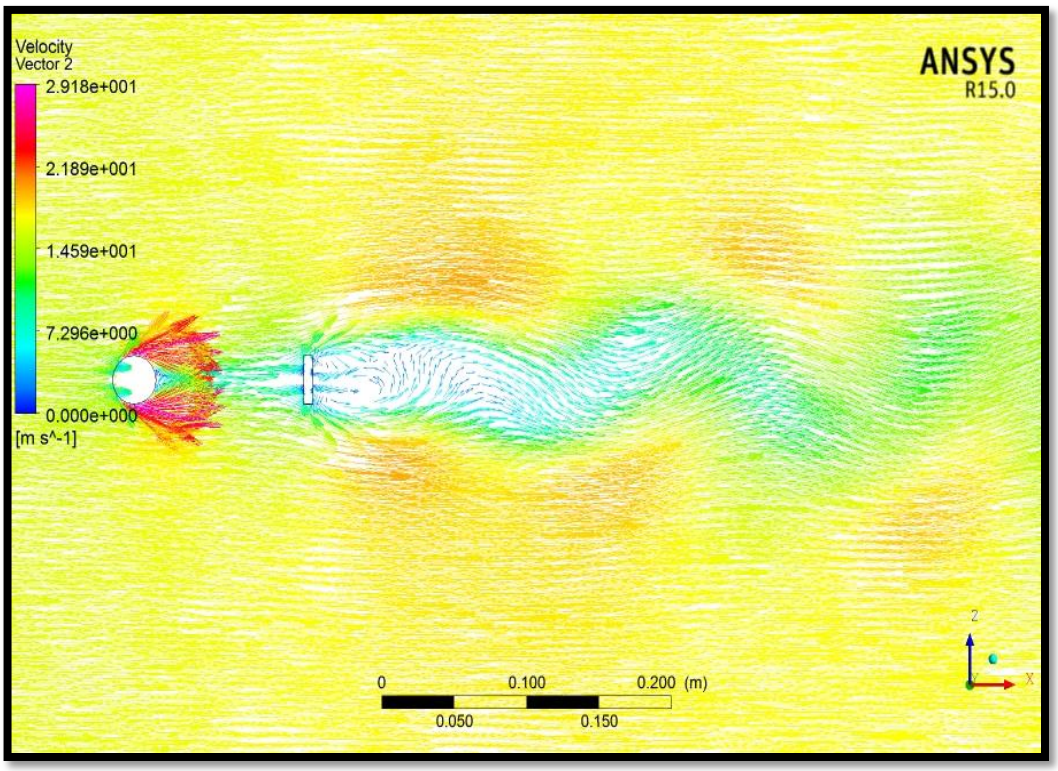

Figure 15. Velocity Vectors at t=0.200001s for $\frac{g}{w} = 4.0$

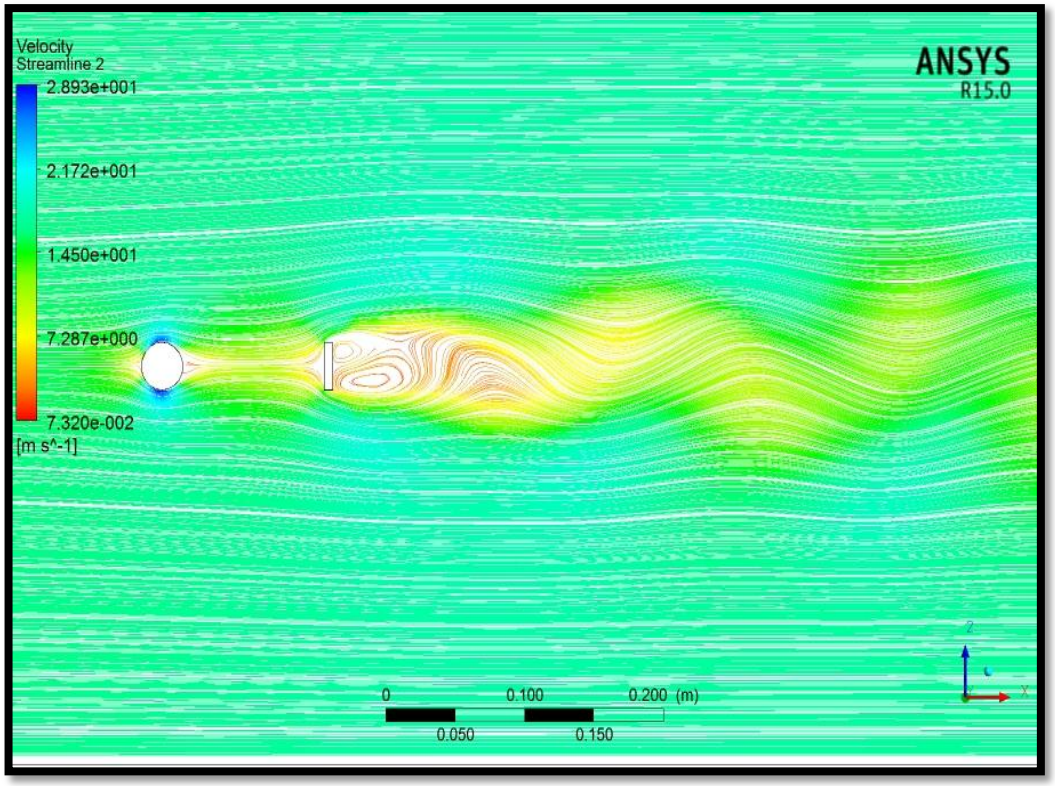

Figure 16. Velocity Streamlines at t=0.200001s for $\frac{g}{w} = \mathbf{4.0}$

By performing FFT on plate lift coefficient the shedding frequency an St number were 64.9194565 (Hz) and 0.1187551 respectively. Figure 16 was generated by performing FFT on C_l. The peak of the power spectral density corresponds to the shedding frequency.

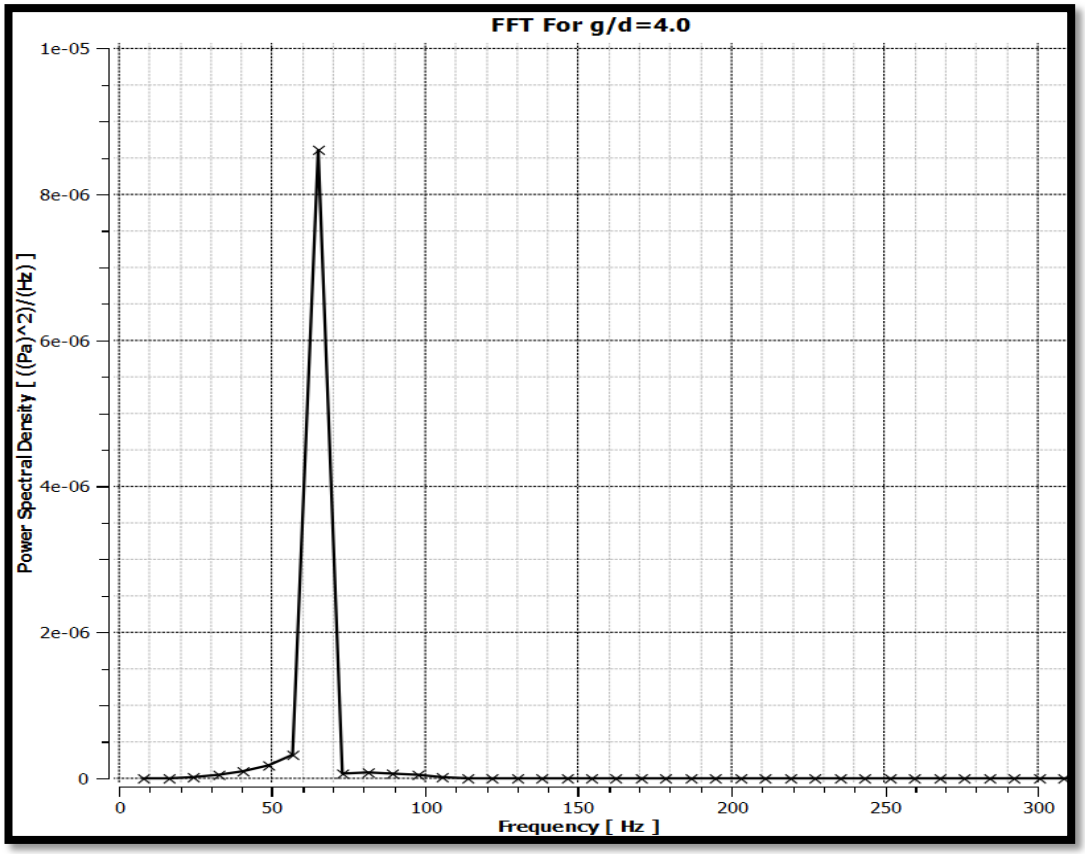

Figure 17. FFT Results for $\frac{g}{w} = \mathbf{4.0}$

4.1.2 Gap Ratio of 3.0

The shedding frequency and St Number for the gap ratio of 3.0 using C_l curve and by performing FFT were 67.5664 (Hz), 65.6565704 (Hz) and 0.1235971, 0.12010348 respectively.

4.1.3 Gap Ratio of 2.0

For the gap ratio of 2.0 again the same contours were drawn. The shedding frequency for this case was 69.94 (Hz) and the St = 0.1270 and the FFT results were 70.7070694 (Hz) and St = 0.1293422.

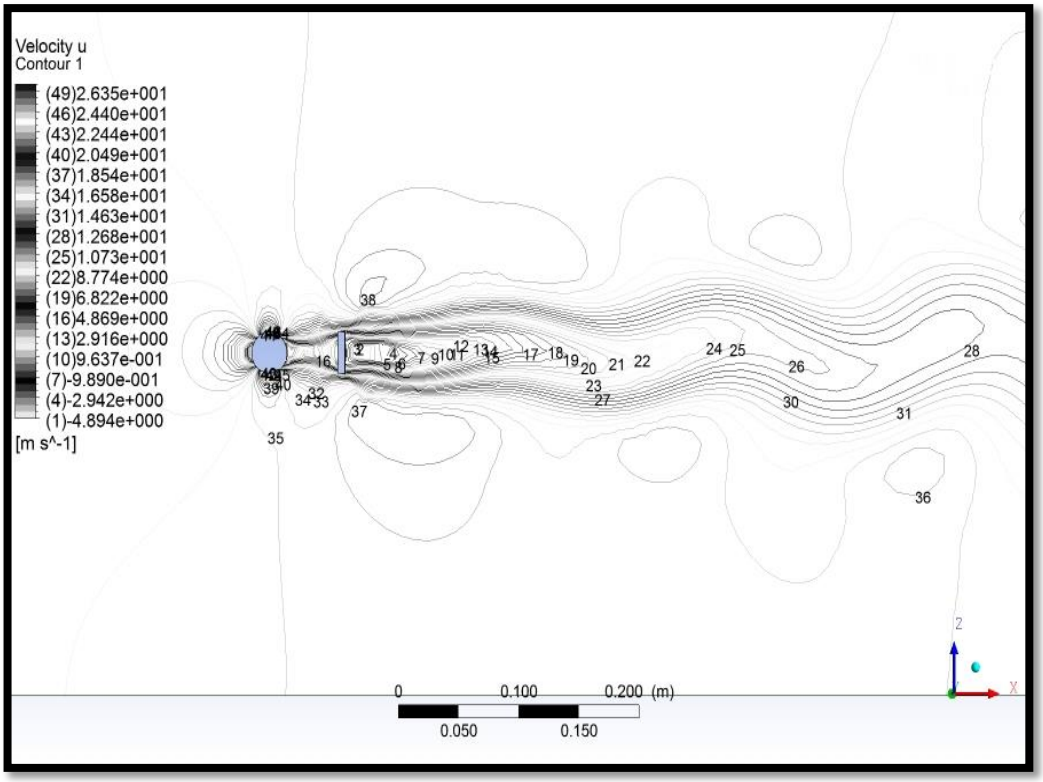

Figure 18. Contours of X-Velocity at t=0.200002s for $\frac{g}{w} = 2.0$

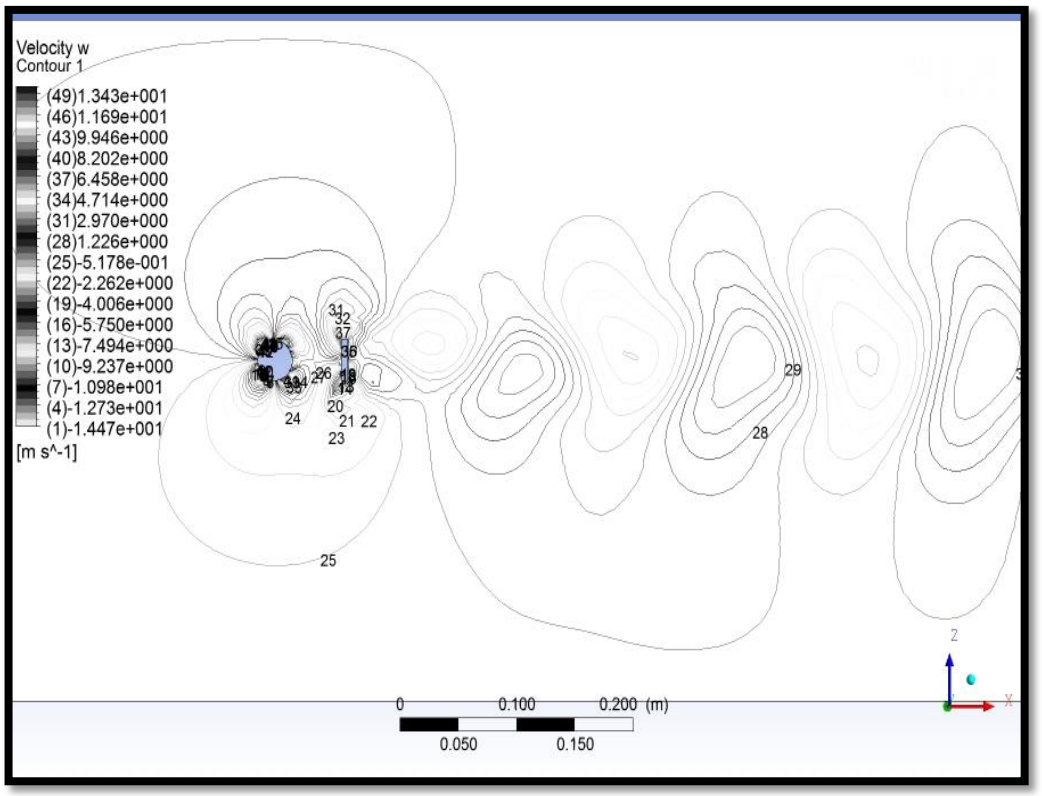

Figure 19. Contours of Z-Velocity at t=0.200002s for $\frac{g}{w} = 2.0$

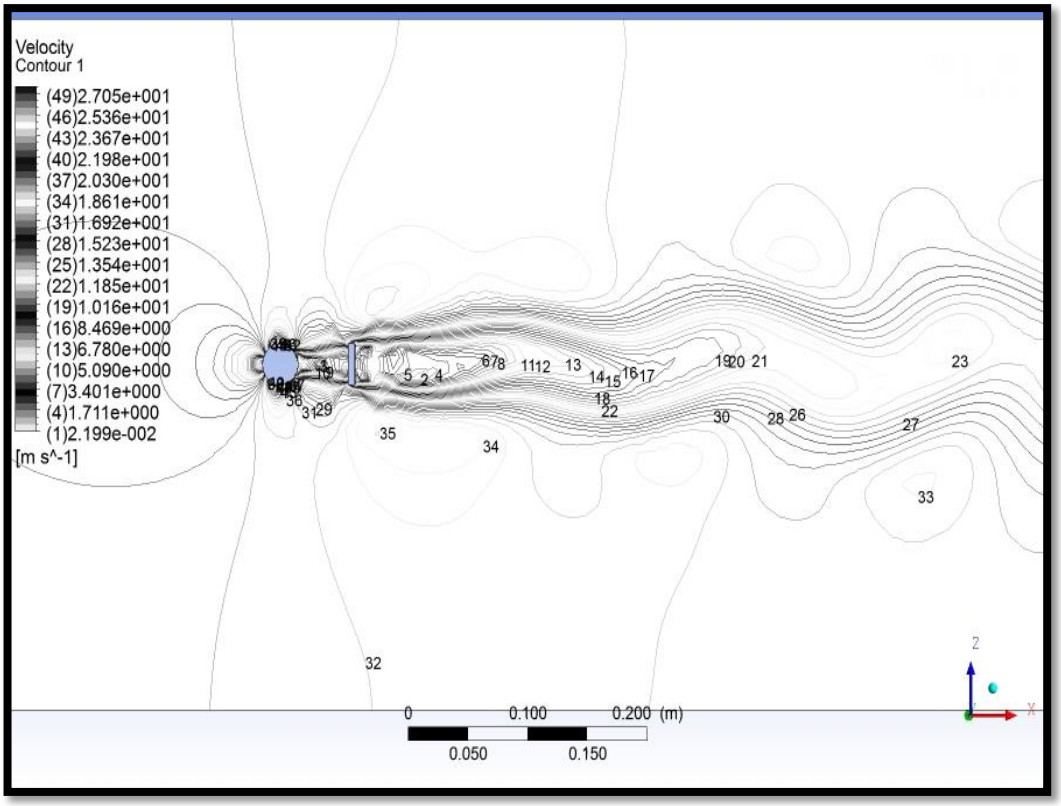

Figure 20. Contours of Velocity at t=0.200002s for $\frac{g}{w} = 2.0$

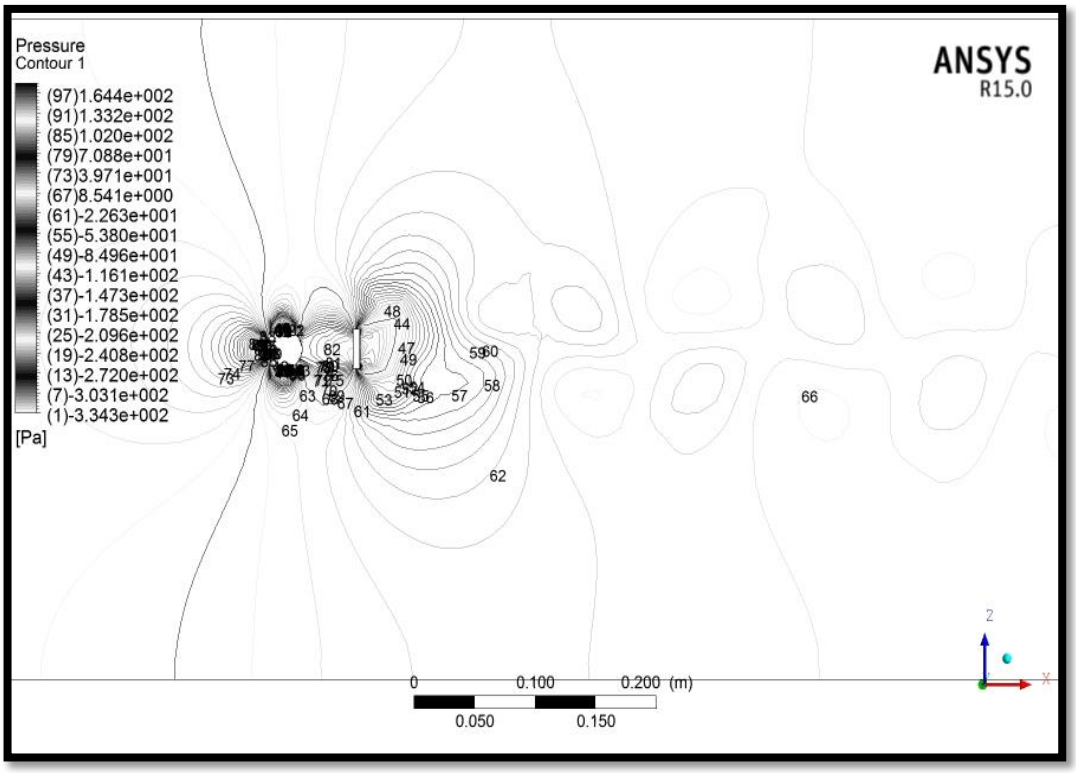

Figure 21. Contours of Pressure at t=0.200002s for $\frac{g}{w} = 2.0$

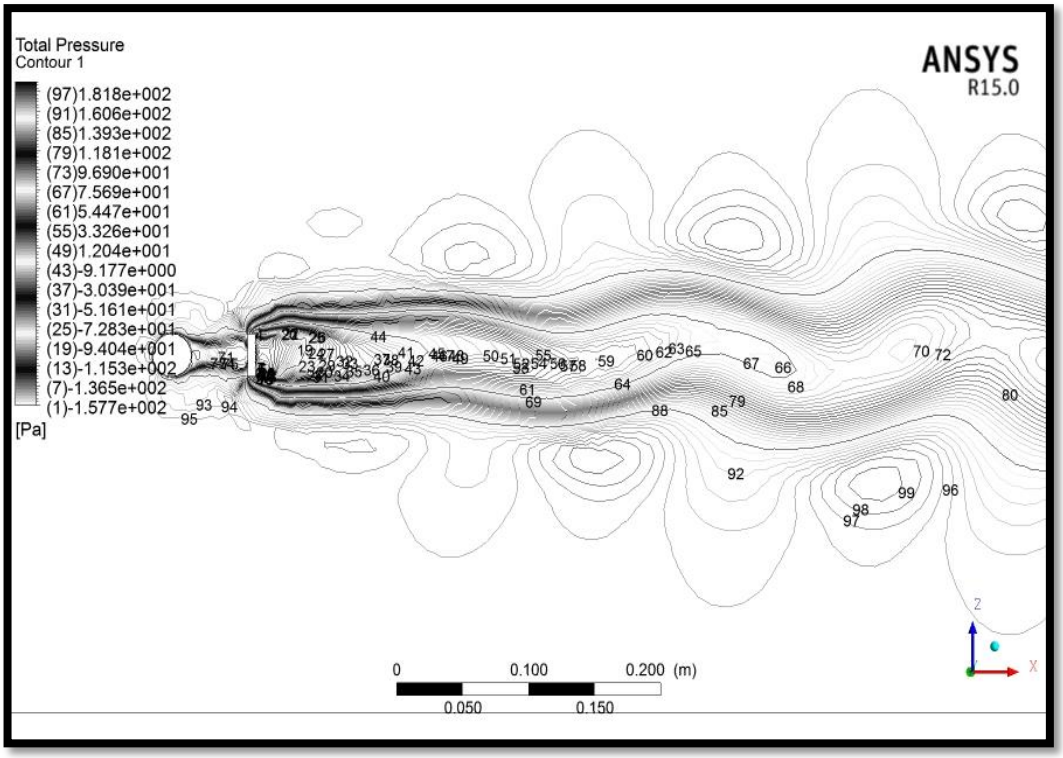

Figure 22. Contours of Total Pressure at t=0.200002s for $\frac{g}{w} = 2.0$

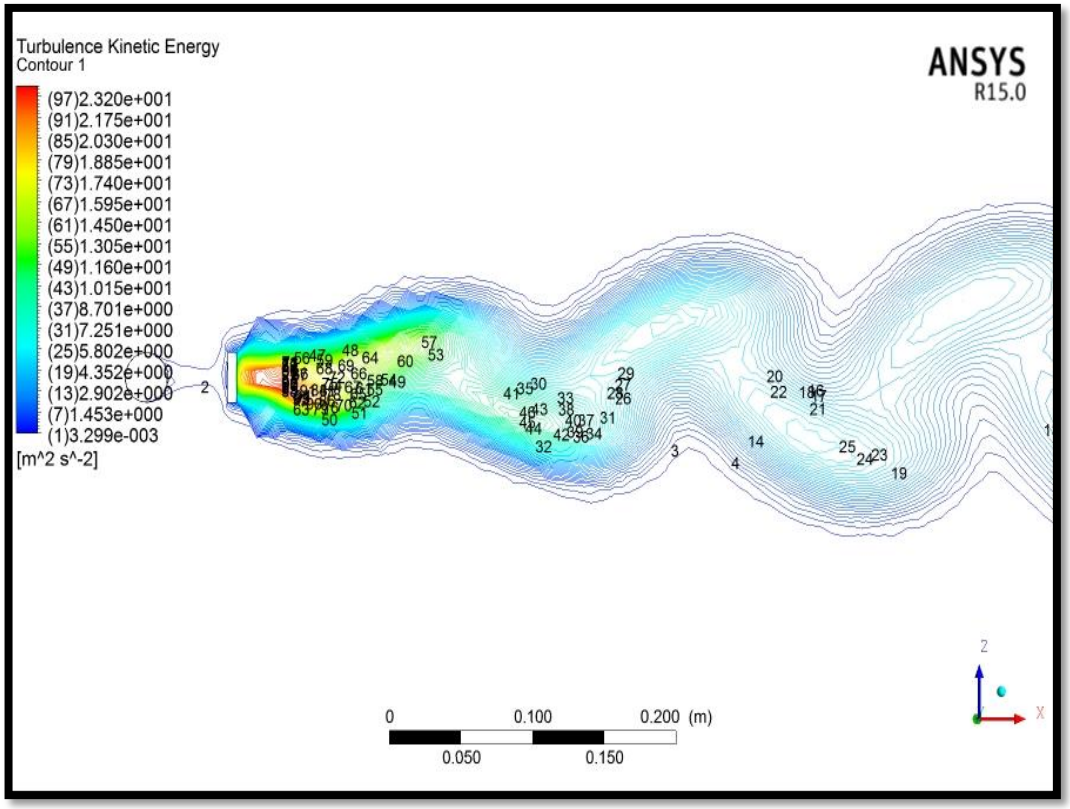

Figure 23. Contours of Turbulence Kinetic Energy at t=0.200002s for $\frac{g}{w} = 2.0$

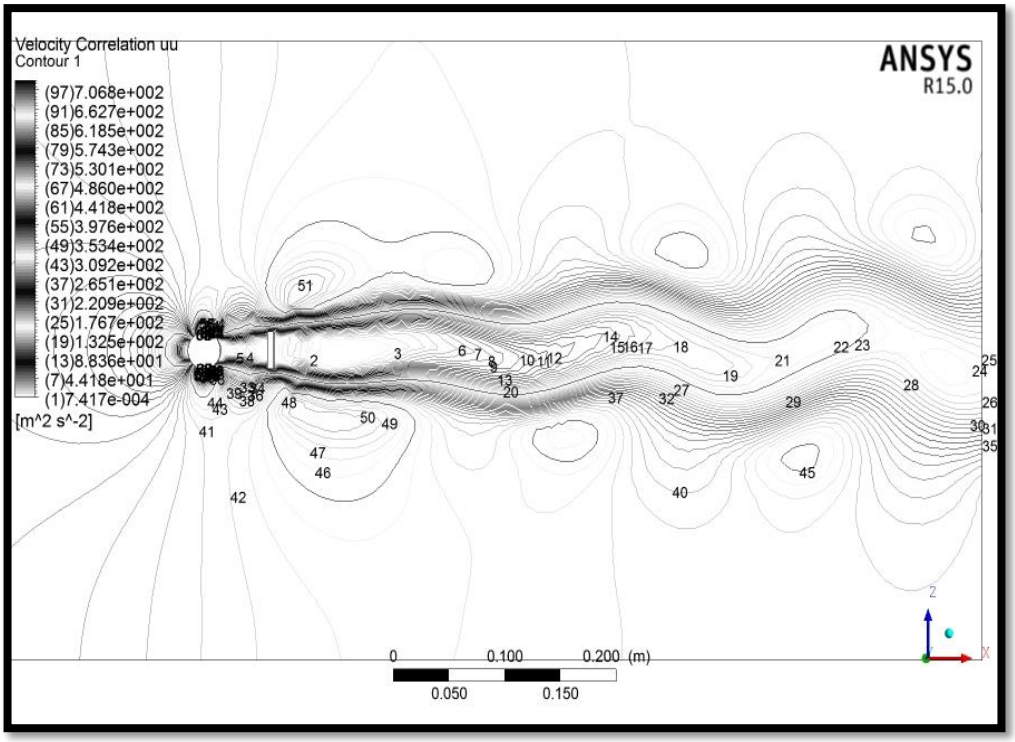

Figure 24. Contours of $u'\,u'$ Velocity at t=0.200002s for $\frac{g}{w} = 2.0$

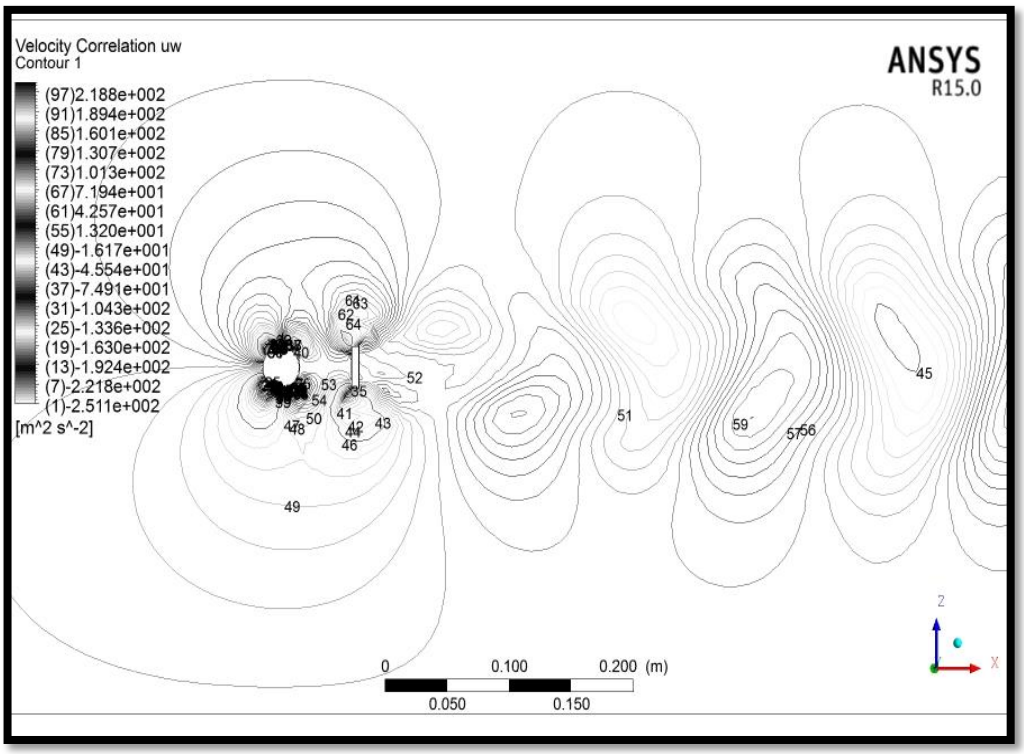

Figure 25. Contours of $u'\,w'$ Velocity at t=0.200002s for $\frac{g}{w} = 2.0$

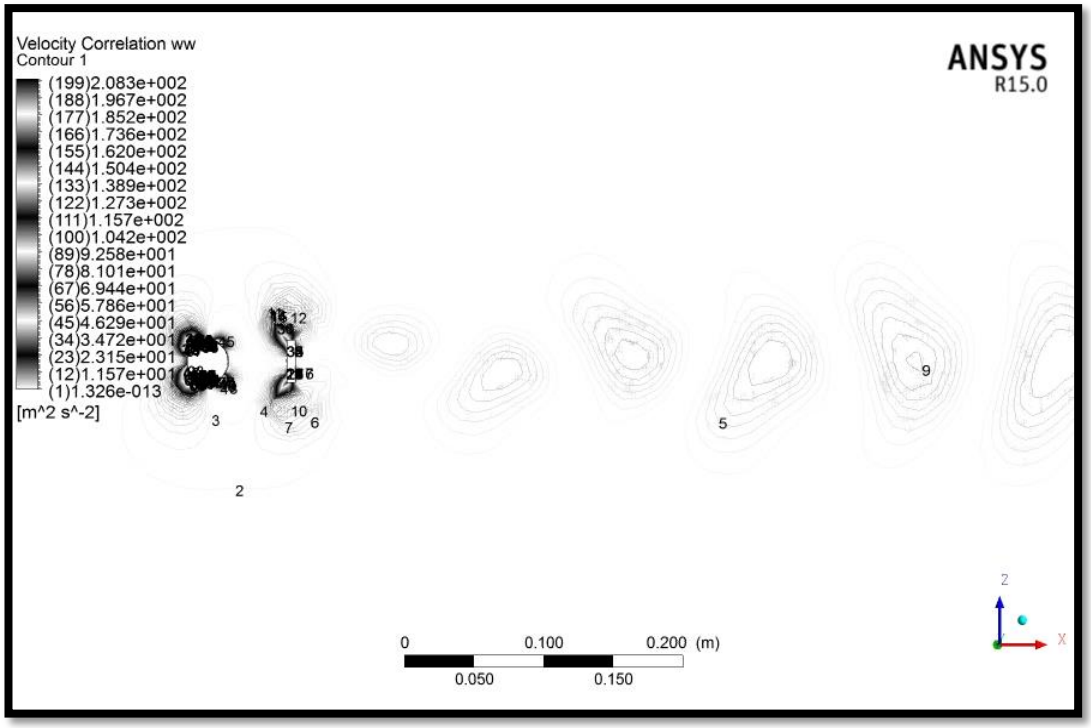

Figure 26. Contours of $w'\,w'$ Velocity at t=0.200002s for $\frac{g}{w} = 2.0$

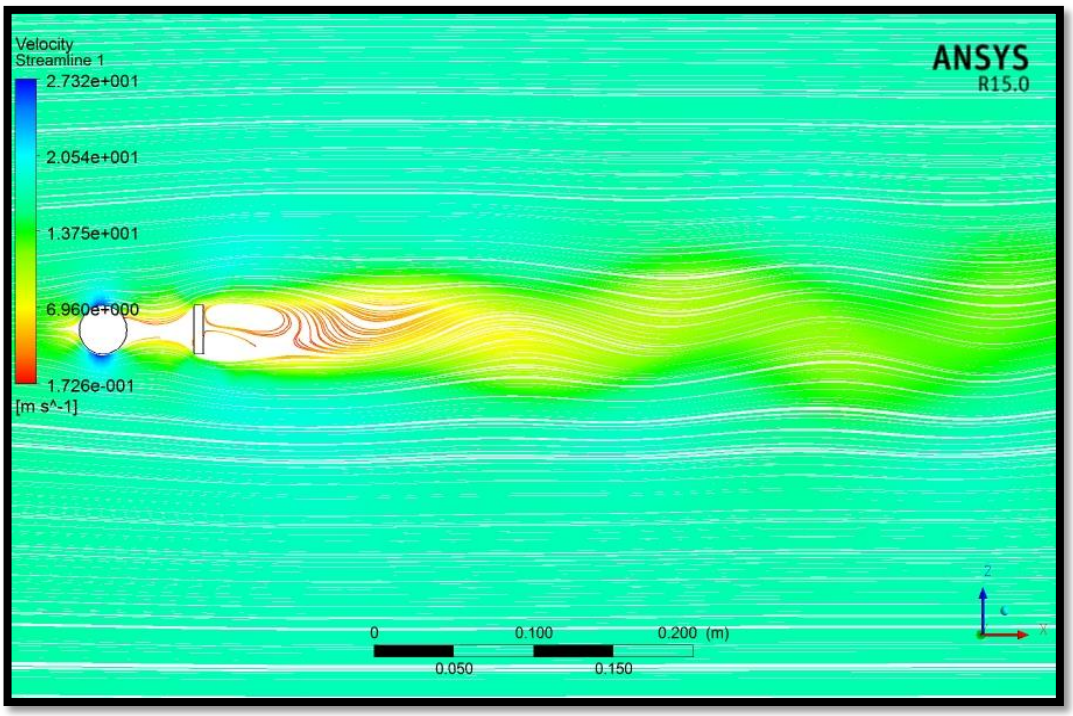

Figure 27. Velocity Streamlines at t=0.200002s for $\frac{g}{w} = 2.0$

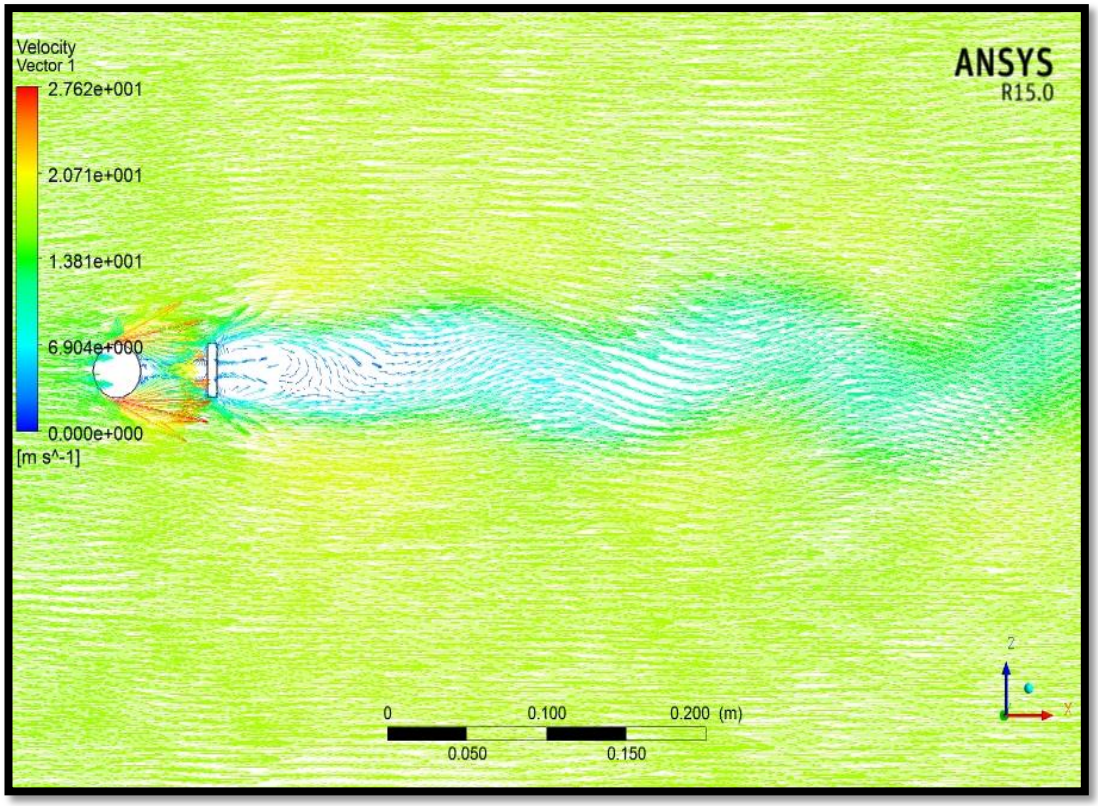

Figure 28. Velocity Vectors at t=0.200002s for $\frac{g}{w} = \mathbf{2.0}$

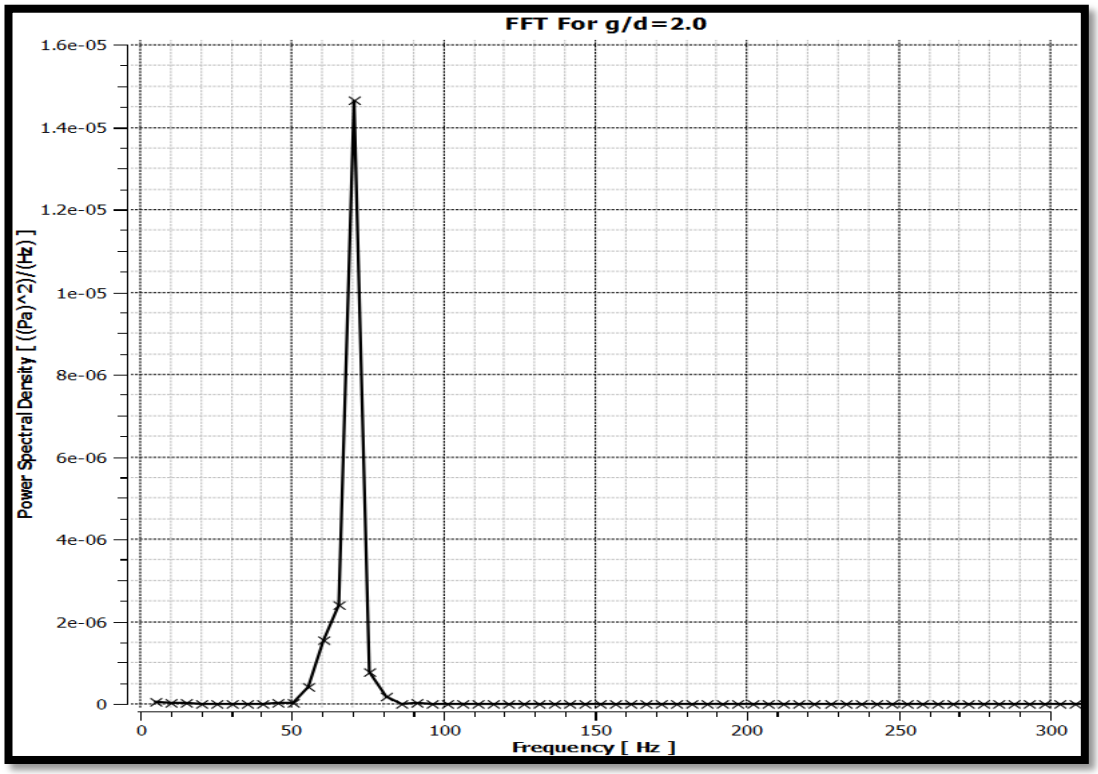

Figure 29. FFT Results for $\frac{g}{w} = \mathbf{2.0}$

4.1.4 Gap Ratio of 1.0

The shedding frequency for this case was 75.7562959 (Hz) and the St = 0.1385786 which showed growth by reducing the gap ratio. The FFT results were 75.757576 (Hz) and 0.13858093 for frequency and St Number respectively.

4.1.5 Gap Ratio of 0.867

The shedding frequency and St Number for the gap ratio of 0.867 using C_l curve and by performing FFT were 78.1237 (Hz), 80.8080826 (Hz) and 0.14291, 0.14781966 respectively.

4.1.6 Gap Ratio of 0.8

Calculated shedding frequency for this case was 79.36 (Hz) which based on the characteristic length gave the St=0.1452. Again the Strouhal number is growing by decreasing the gap ratio. The FFT results were f = 80.8080826 (Hz) and St = 0.14781966, which were the same as previous gap ratio.

4.2 Representation of 30 (*mm*) Wide Plate and 15 (*mm*) Diameter Circular Cylinder

For the gap ratios of 1.0 and 0.8 the X and Z velocity, velocity, pressure, total pressure, turbulence kinetic energy, $u'u', u'w', w'w'$ velocity correlations contours are illustrated. For gap ratios of 2.0, 3.0 and 4.0 only calculated shedding frequency and Strouhal number are reported.

4.2.1 Gap Ratio of 4.0

Calculated shedding frequency for this case was 65.7884 (Hz) which based on the characteristic length of the plate and the St=0.1203446 which is higher than the same gap ratio cylinder and plate but with *w/d=1.0*.

4.2.2 Gap Ratio of 3.0

The shedding frequency for this case was 66.6655 (Hz) and the St = 0.1219491 which has been grown by reducing the gap ratio. The FFT results were 65.5772781 (Hz) and 0.11995844 for frequency and St Number respectively.

4.2.3 Gap Ratio of 2.0

For the gap ratio of two the shedding frequency from the plate and the Strouhal number were 67.5664 (Hz) and 0.1235971 respectively. The shedding frequency and as a result the Strouhal number increased with respect to the gap ratio of 4.0 for these geometries but decreased with respect to same gap ratio and *w/d*=1.0. FFT results were *f* = 65.6565704 (Hz) and St = 0.12010348.

4.2.4 Gap Ratio of 1.0

The X and Z velocity, velocity, pressure, total pressure, turbulence kinetic energy, $u'u', u'w', w'w'$ velocity correlations contours for the gap ratio of 1.0 were illustrated. The shedding frequency and Strouhal numbers were 73.5282 (Hz) and 0.1345028, respectively. Similar to the previous case study, the frequency and St number both increase with decreasing the center to center distance but decreased compare to the same gap ratio but *w/d=1.0*. FFT results were *f* = 74.6960144 (Hz) and St = 0.13663905.

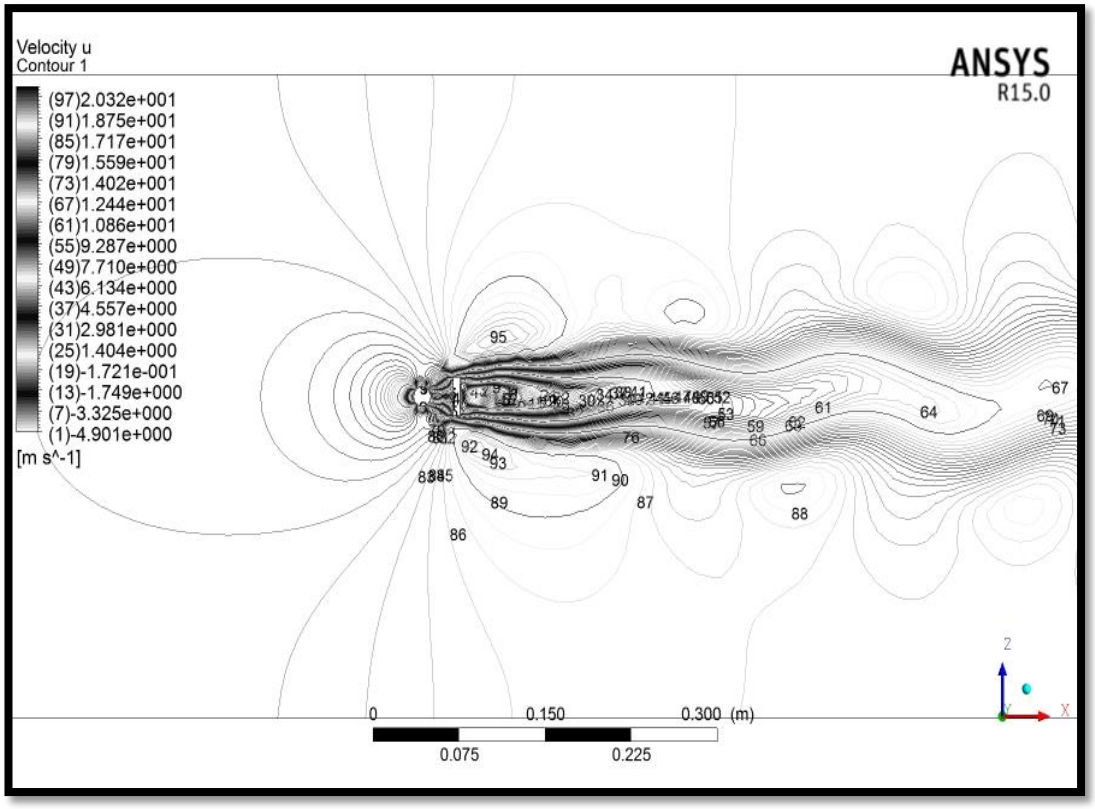

Figure 30. Contours of X-Velocity at t=0.200002s for $\frac{g}{w} = 1.0$

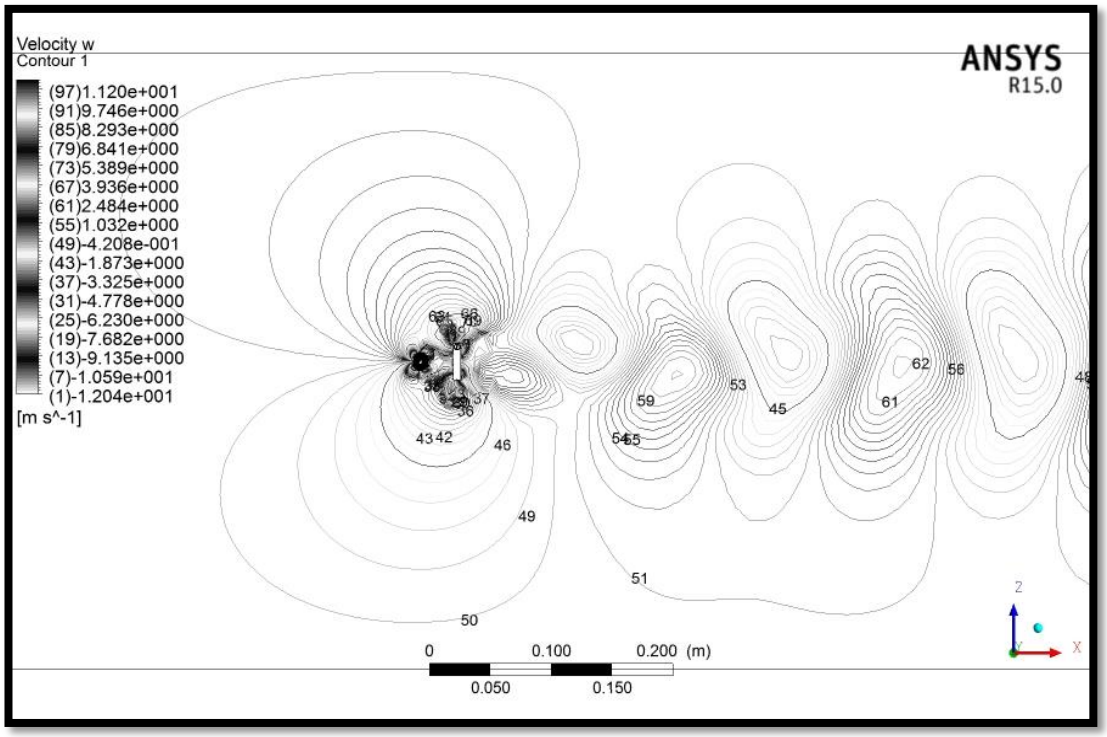

Figure 31. Contours of Z-Velocity at t=0.200002s for $\frac{g}{w} = 1.0$

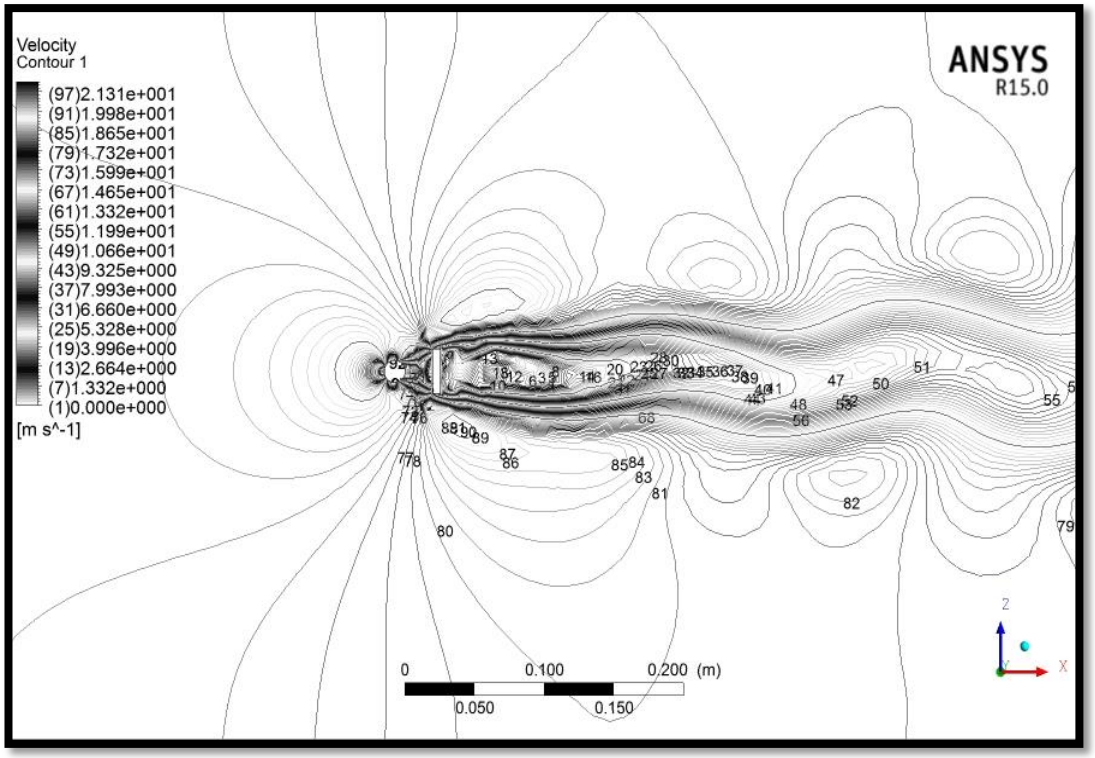

Figure 32. Contours of Z-Velocity at t=0.200002s for $\frac{g}{w} = 1.0$

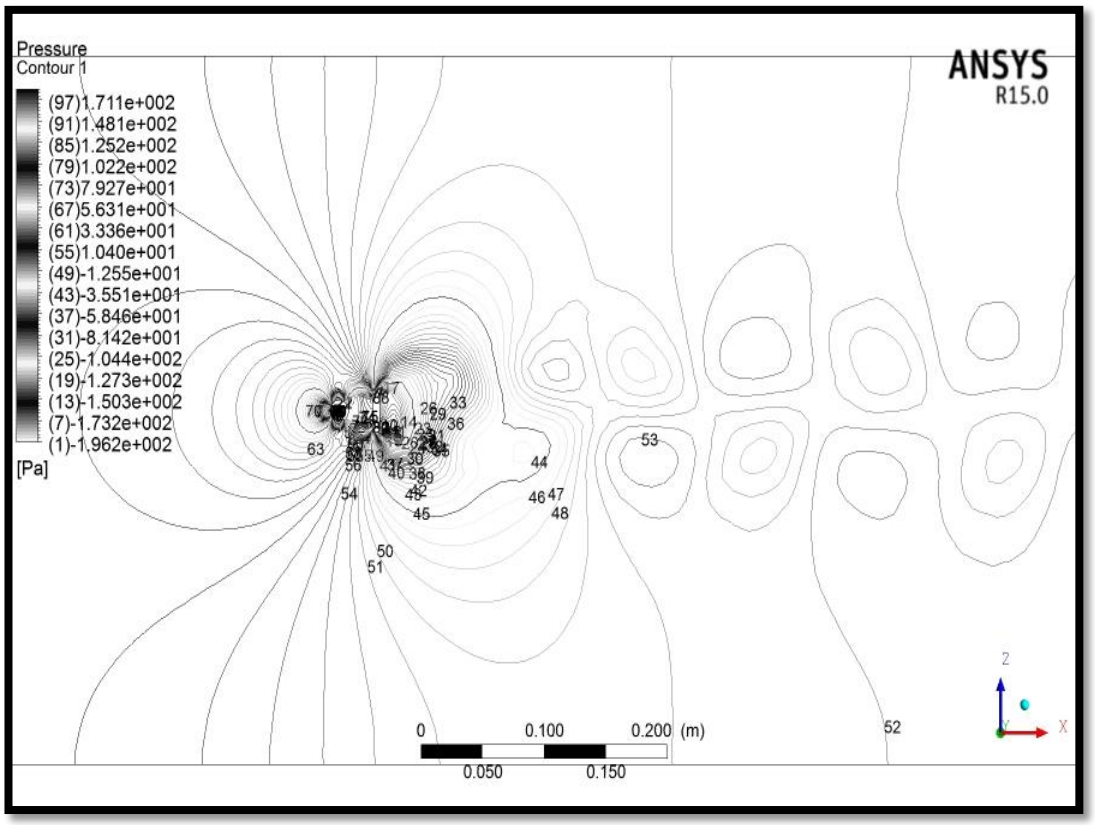

Figure 33. Contours of Pressure at t=0.200002s for $\frac{g}{w} = 1.0$

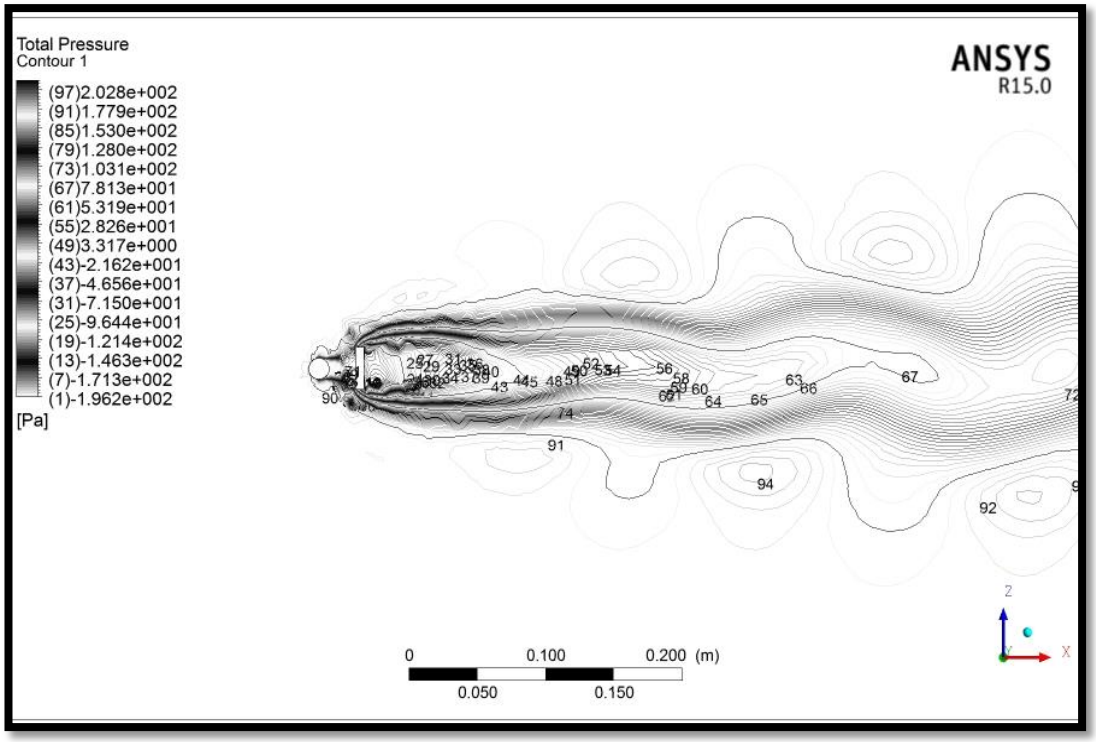

Figure 34. Contours of Total Pressure at t=0.200002s for $\frac{g}{w} = 1.0$

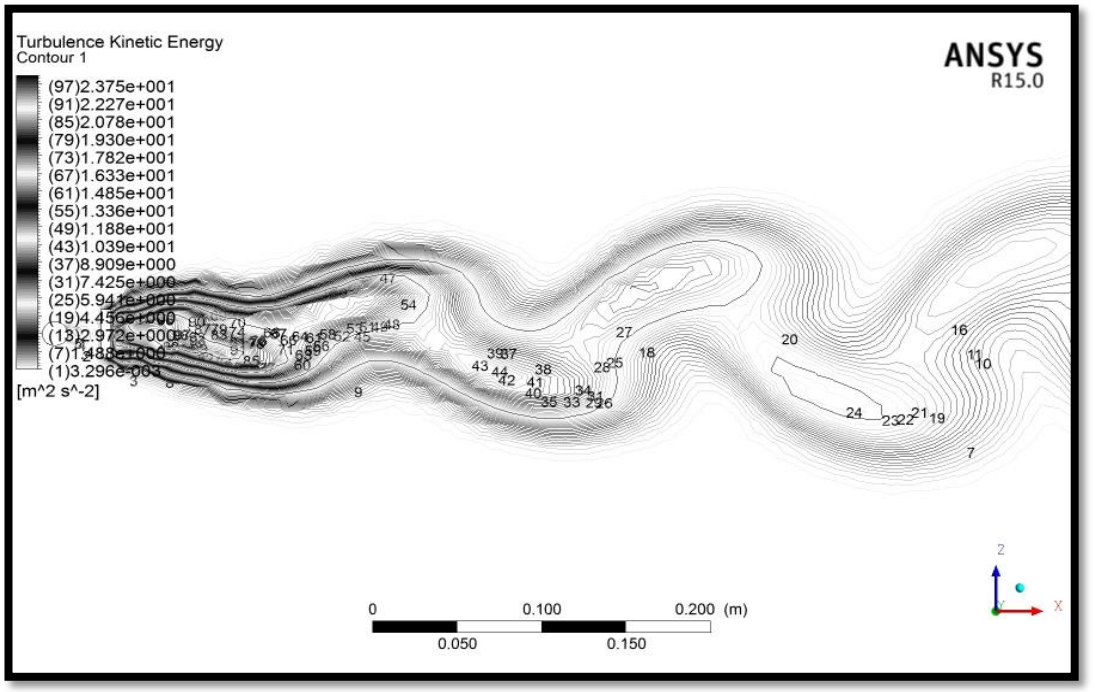

Figure 35. Contours of Turbulence Kinetic Energy at t=0.200002s for $\frac{g}{w} = 1.0$

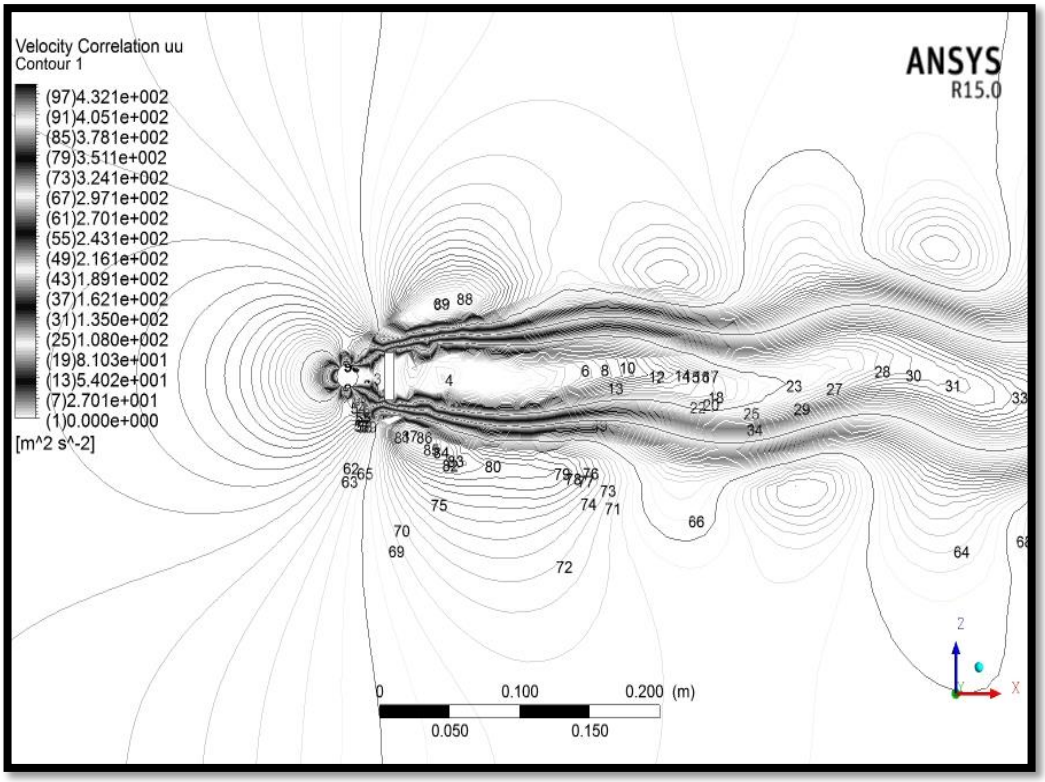

Figure 36. Contours of $u'\,u'$ Velocity at t=0.200002s for $\frac{g}{w} = 1.0$

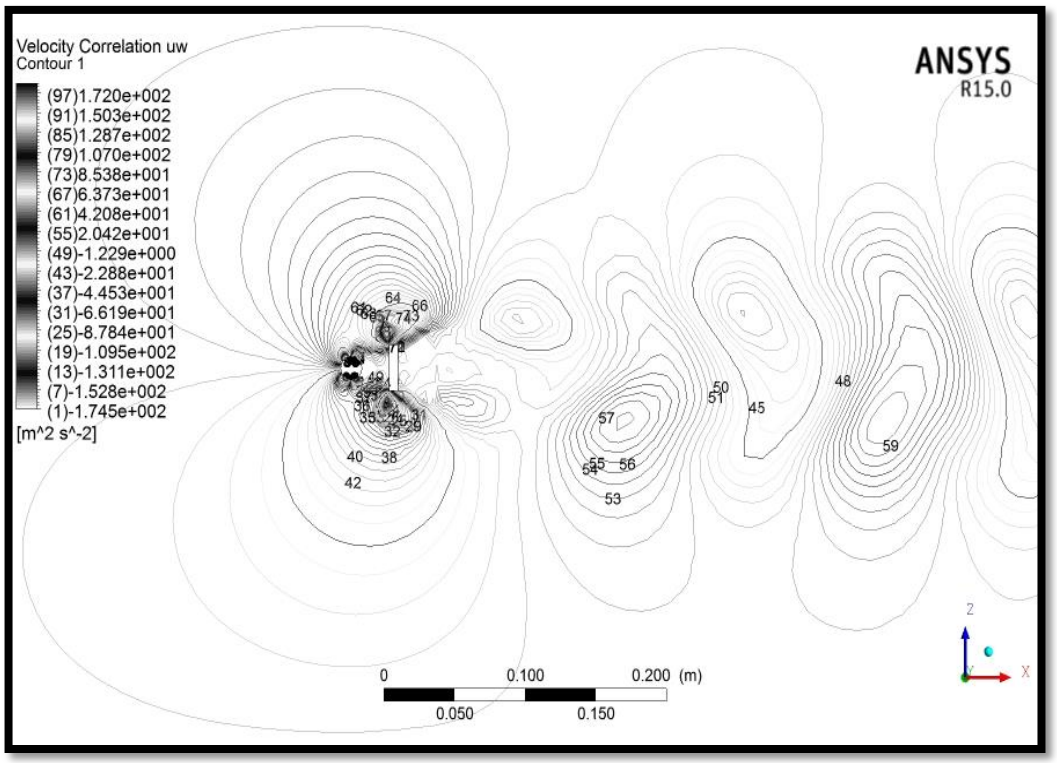

Figure 37. Contours of $u'\,w'$ Velocity at t=0.200002s for $\frac{g}{w} = 1.0$

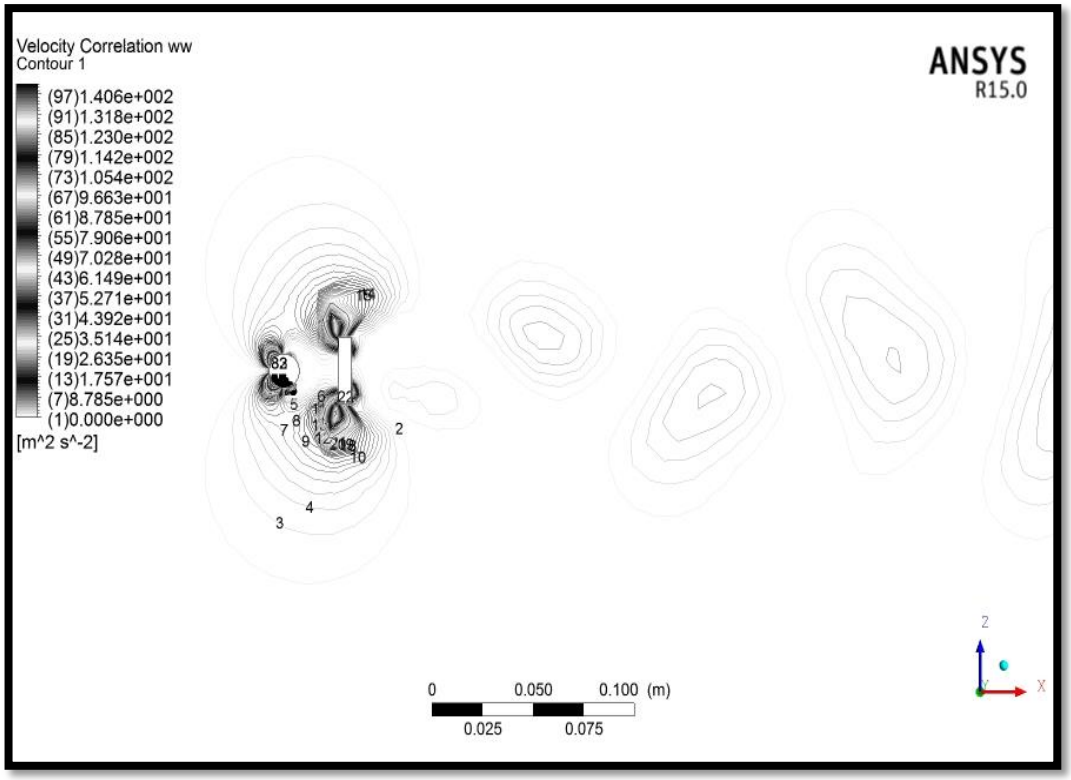

Figure 38. Contours of $w'\,w'$ Velocity at t=0.200002s for $\frac{g}{w} = 1.0$

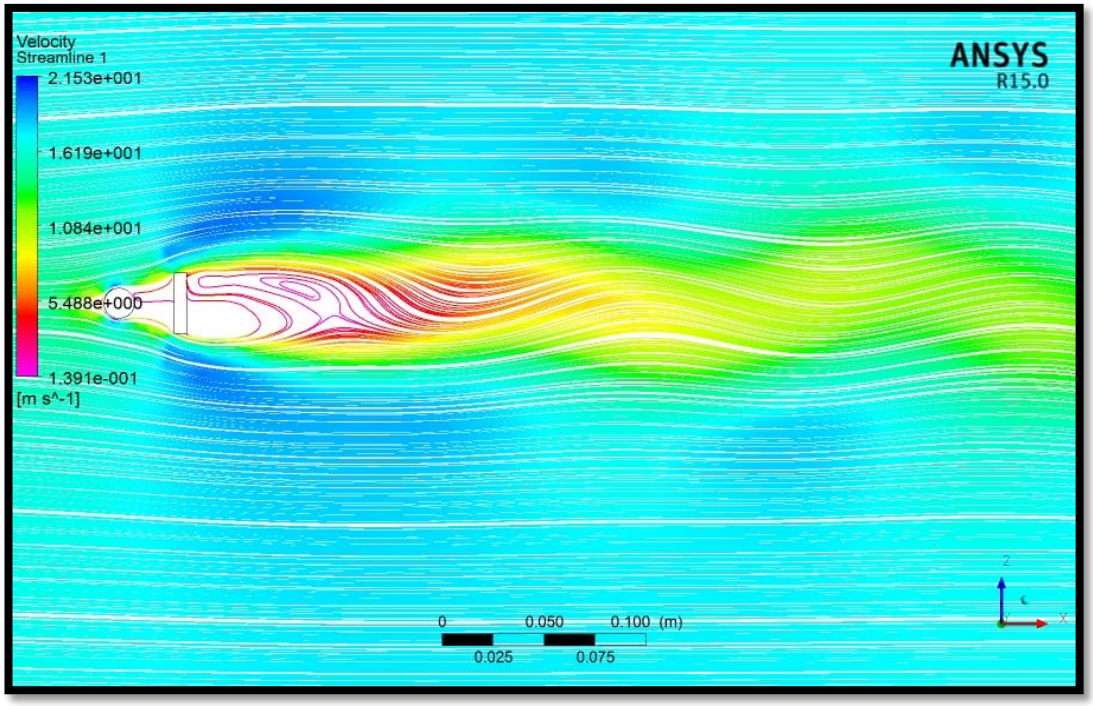

Figure 39. Velocity Streamlines at t=0.200002s for $\frac{g}{w} = 1.0$

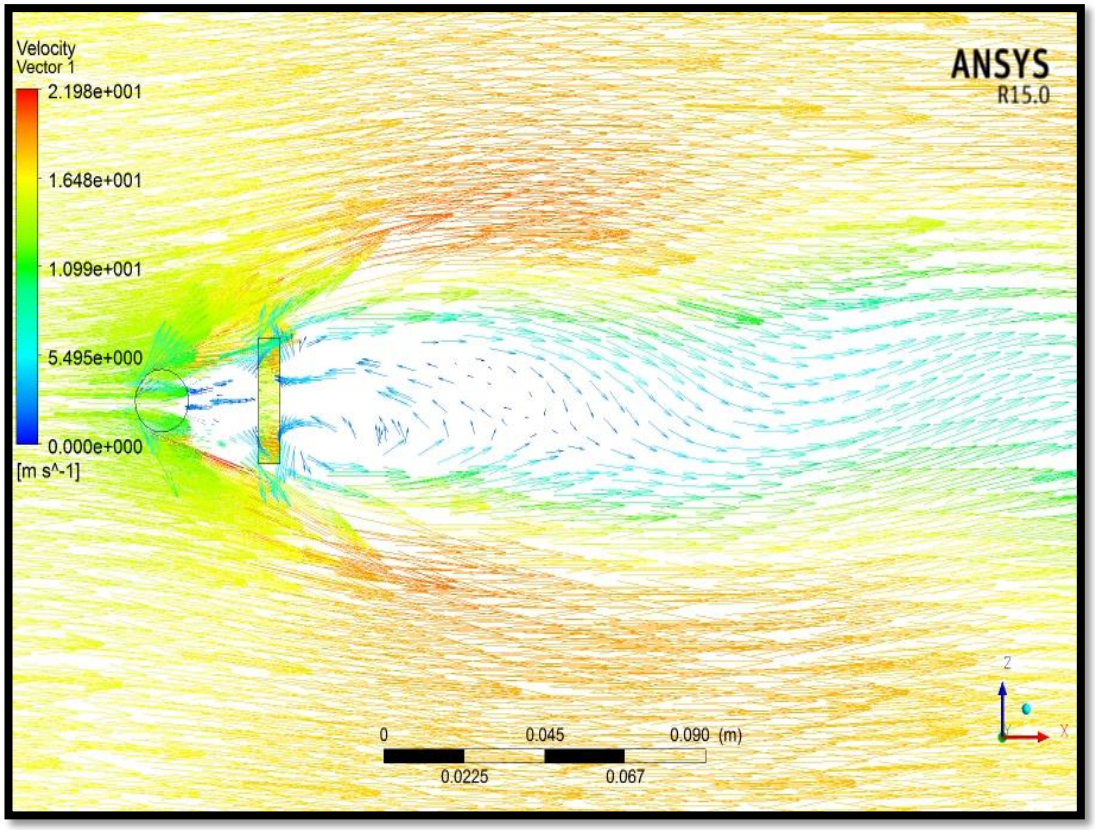

Figure 40. Velocity Vectors at t=0.200002s for $\frac{g}{w} = \mathbf{1.0}$

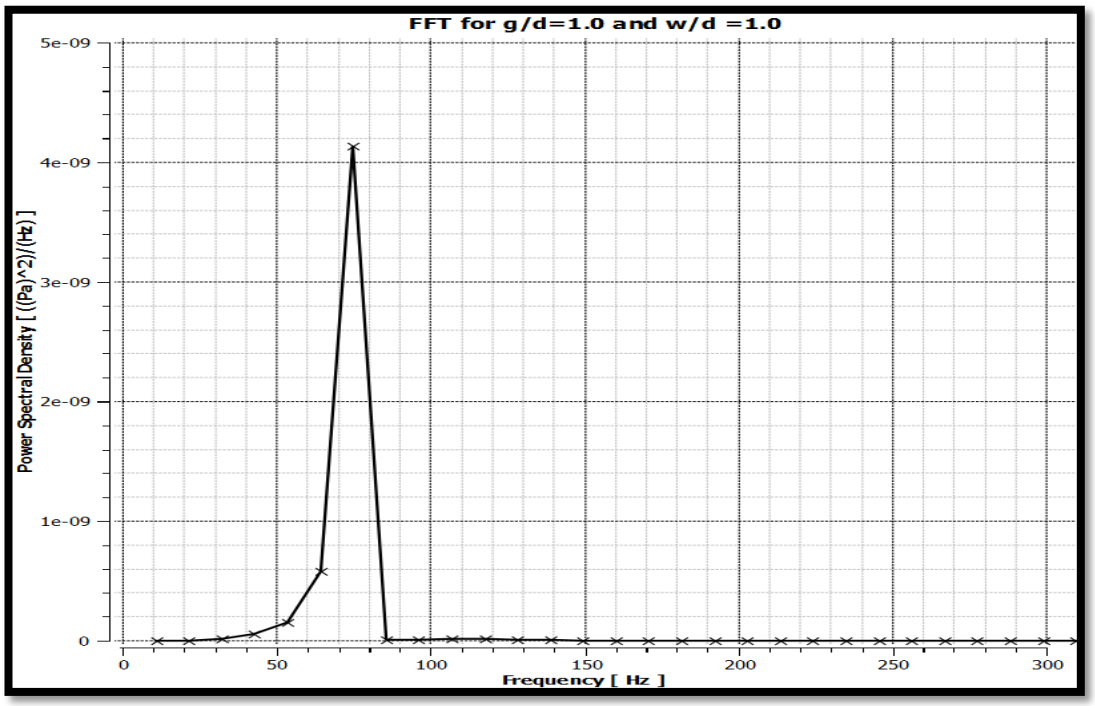

Figure 41. FFT Results for $\frac{g}{w} = \mathbf{1.0}$ and w/d=1.0

4.2.5 Gap Ratio of 0.867

The shedding frequency and St Number for the gap ratio of 0.867 using C_l curve and by performing FFT were 76.9218 (Hz), 75.6660919 (Hz) and 0.1407106, 0.13841358 respectively.

4.2.6 Gap Ratio of 0.8

The X and Z velocity, velocity, pressure, total pressure, turbulence kinetic energy, $u'u', u'w', w'w'$ velocity correlations contours for the gap ratio of 0.8 were illustrated. The shedding frequency and Strouhal numbers were 76.9218 (Hz) and 0.1407106 respectively. Similar to the previous case study, the frequency and St number both increase with decreasing the gap ratio but decreased compare to the same gap ratio but *w/d=1.0*. FFT results were f = 75.757576 (Hz) and St = 0.13858093.

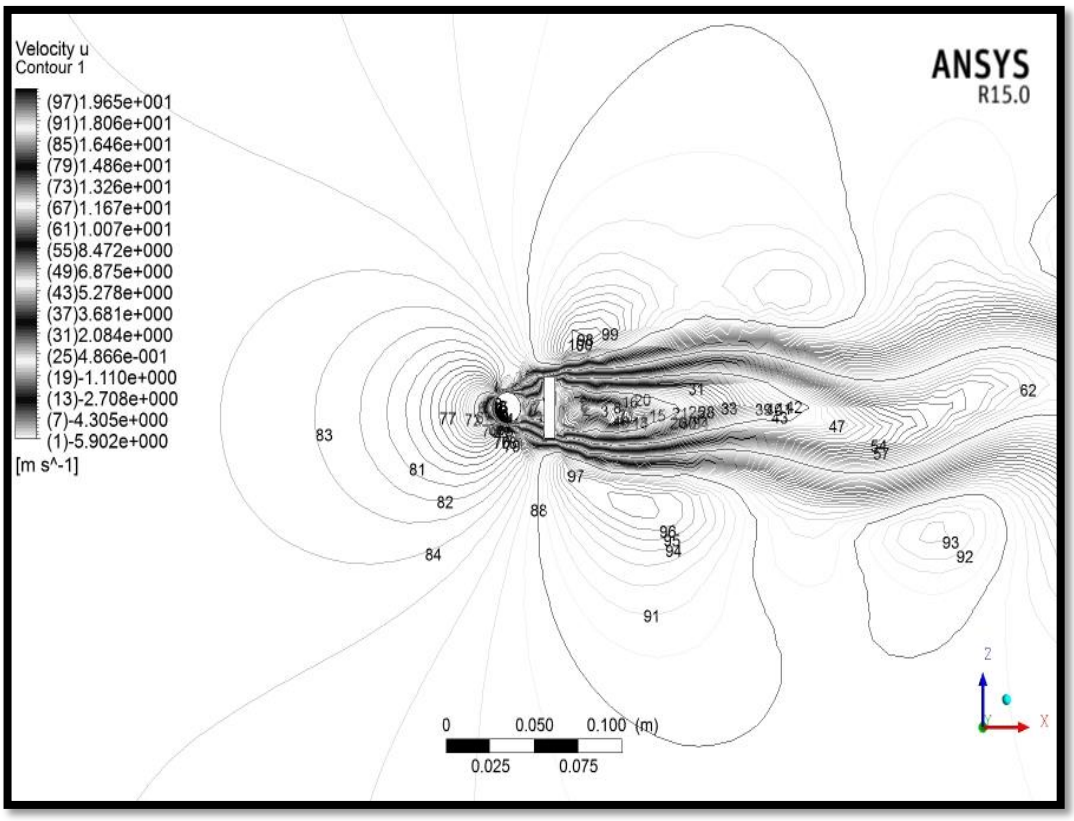

Figure 42. Contours of X-Velocity at t=0.200002s for $\frac{g}{w} = 0.8$

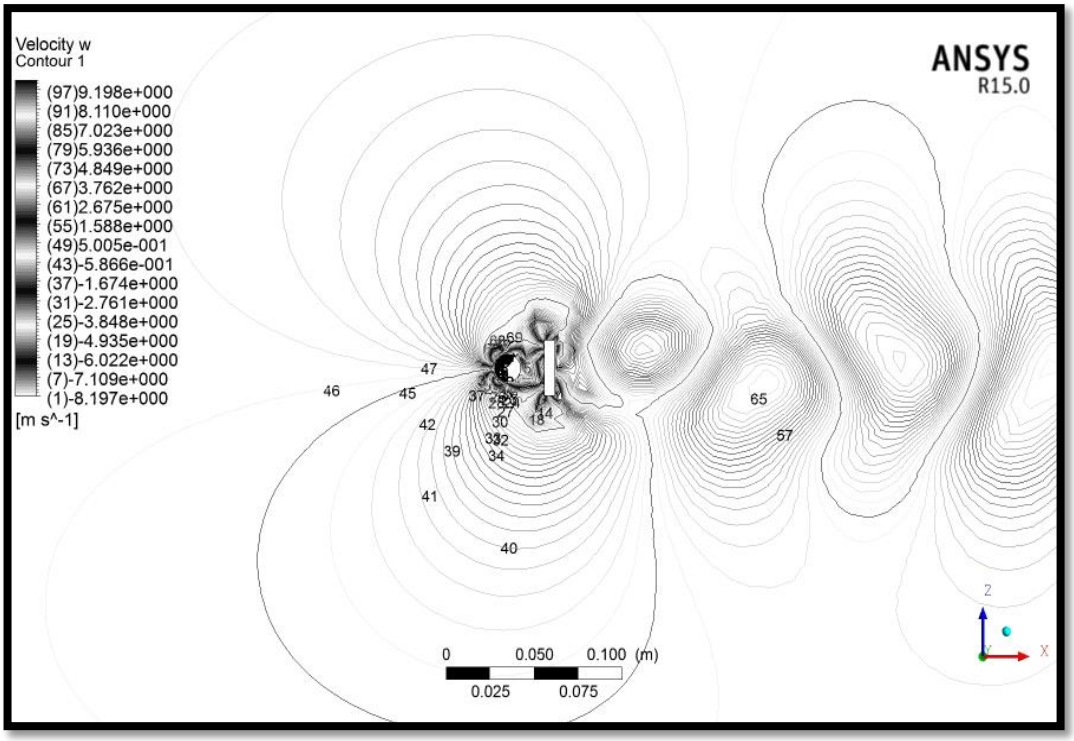

Figure 43. Contours of Z-Velocity at t=0.200002s for $\frac{g}{w} = 0.8$

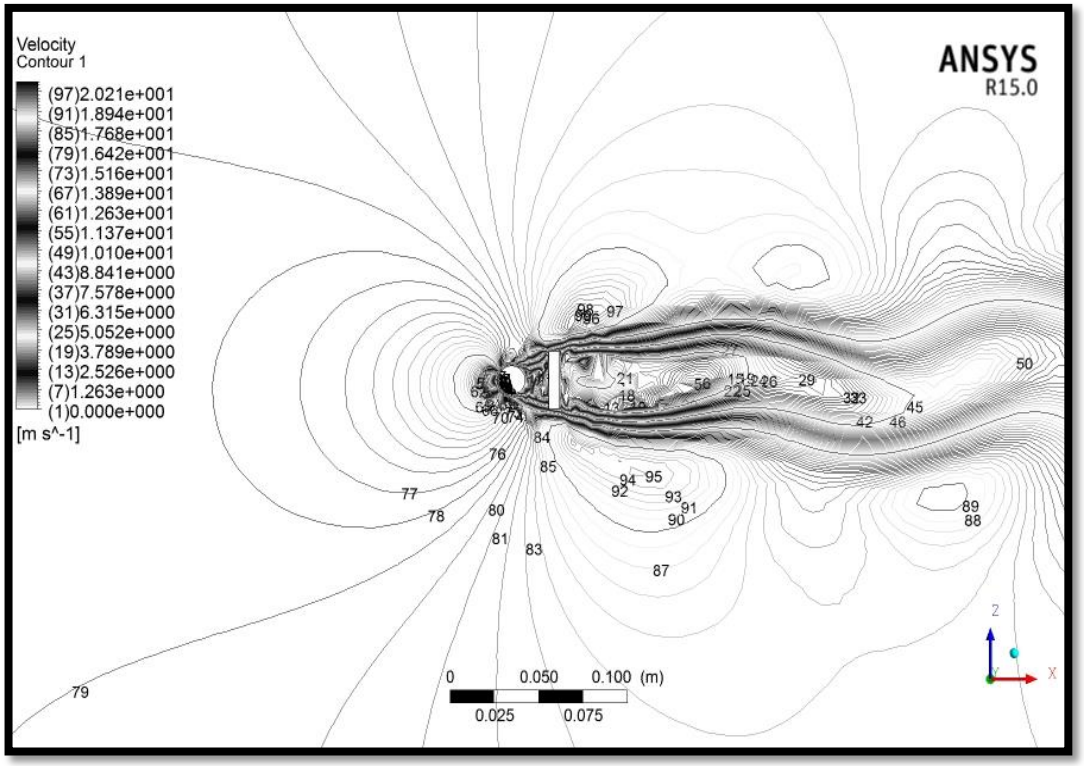

Figure 44. Contours of Velocity at t=0.200002s for $\frac{g}{w} = 0.8$

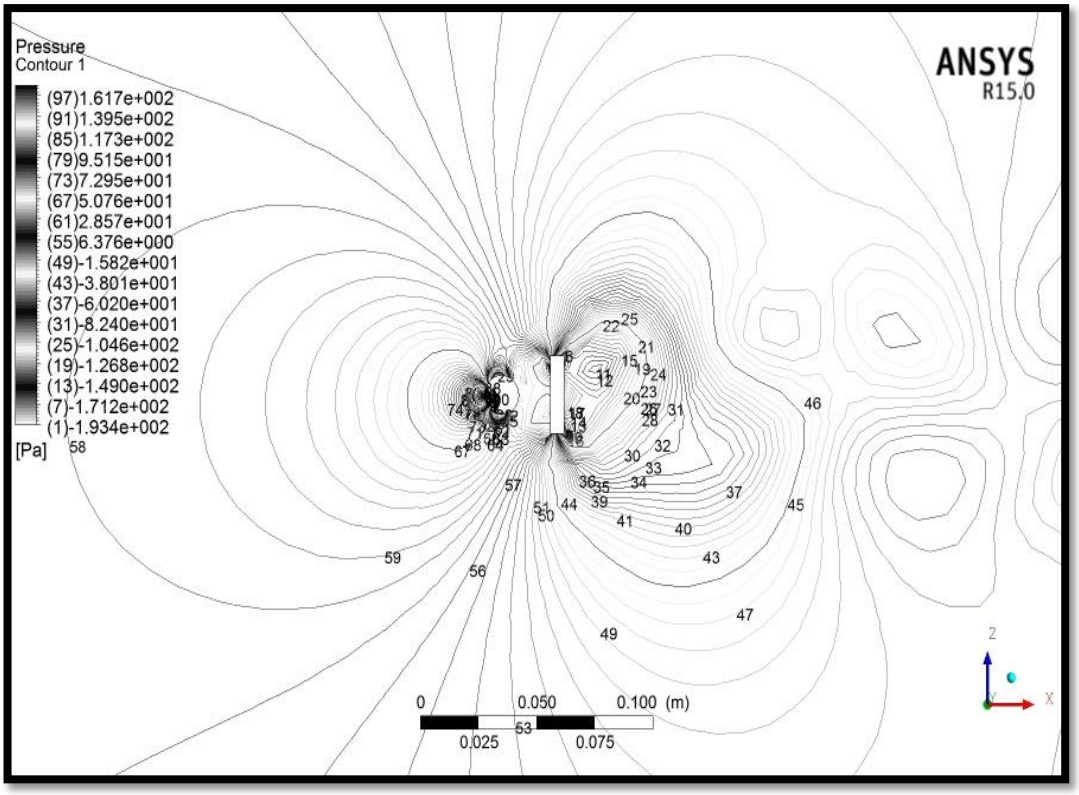

Figure 45. Contours of Pressure at t=0.200002s for $\frac{g}{w} = 0.8$

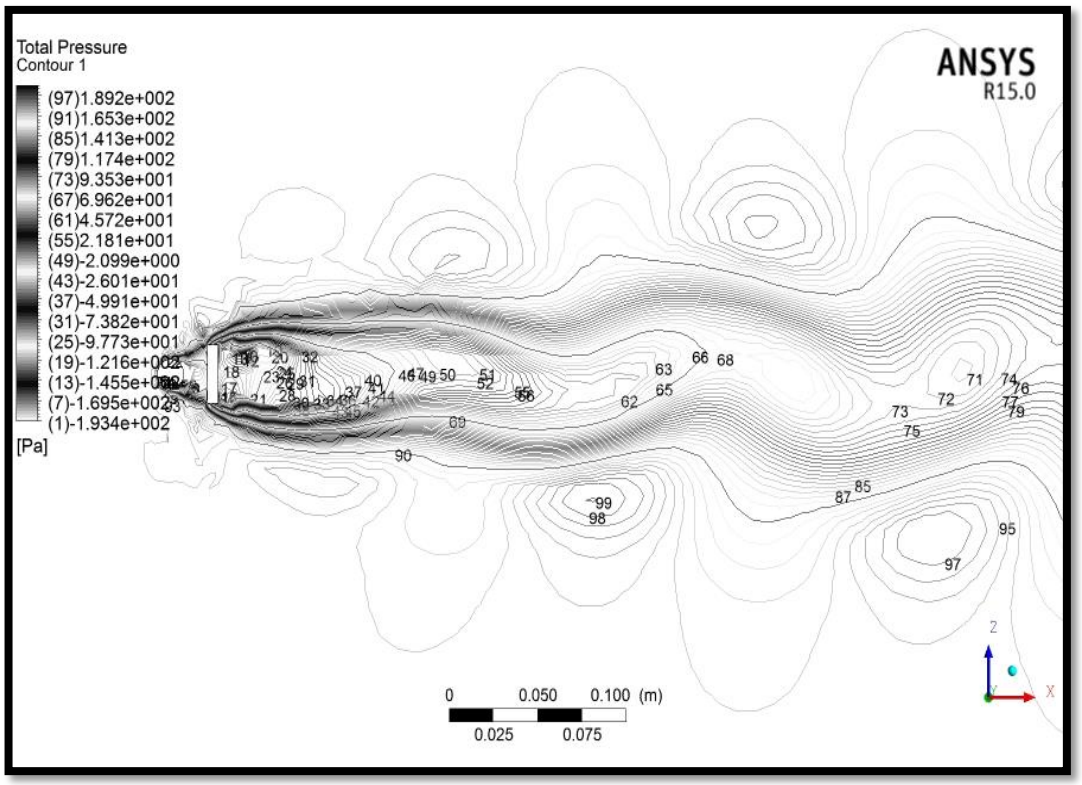

Figure 46. Contours of Total Pressure at t=0.200002s for $\frac{g}{w} = 0.8$

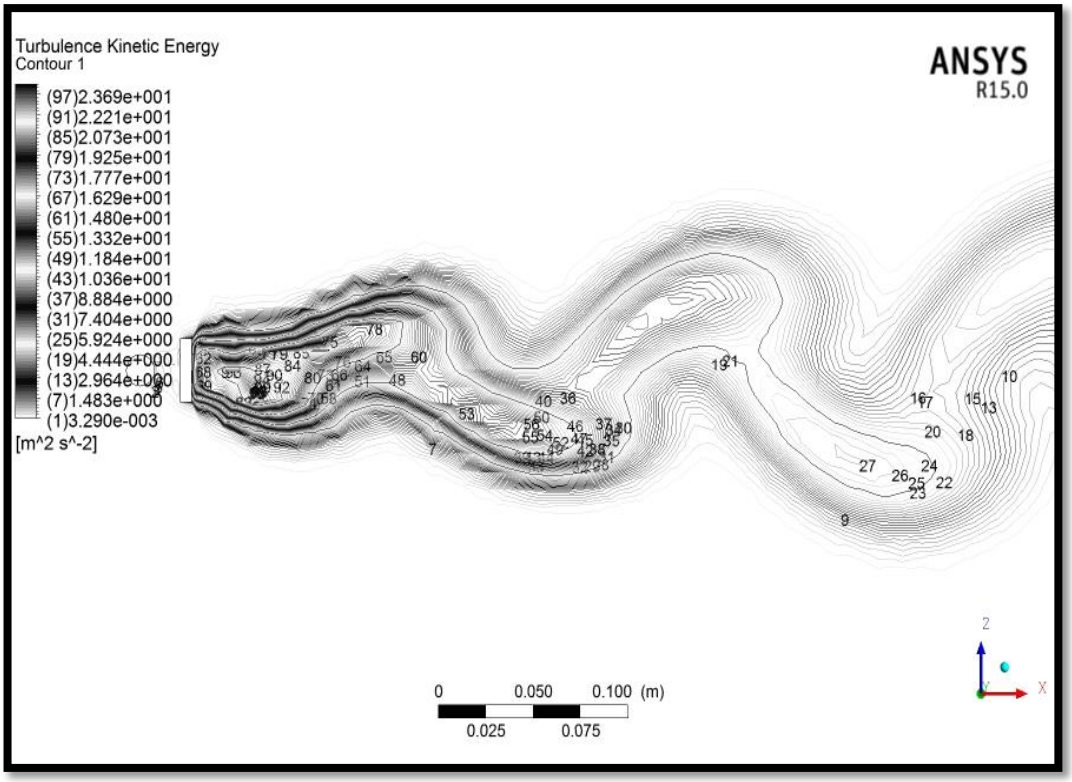

Figure 47. Contours of Turbulence Kinetic Energy at t=0.200002s for $\frac{g}{w} = 0.8$

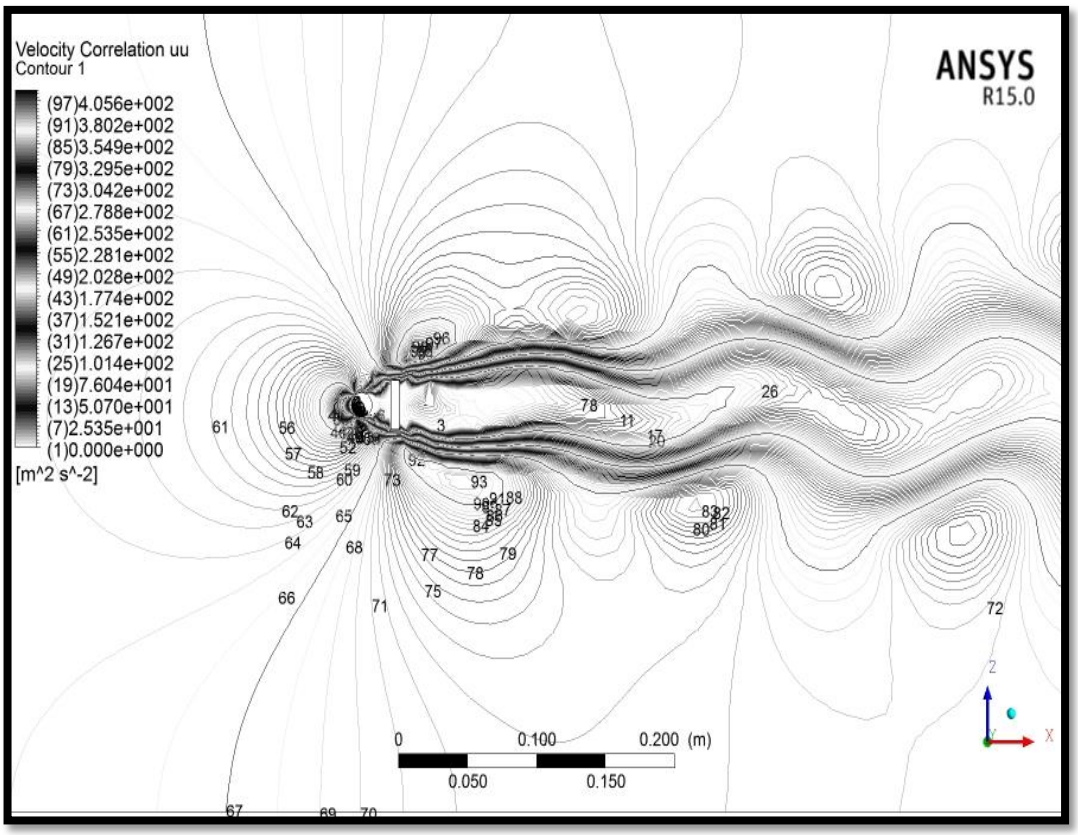

Figure 48. Contours of $u'\,u'$ Velocity at t=0.200002s for $\frac{g}{w} = 0.8$

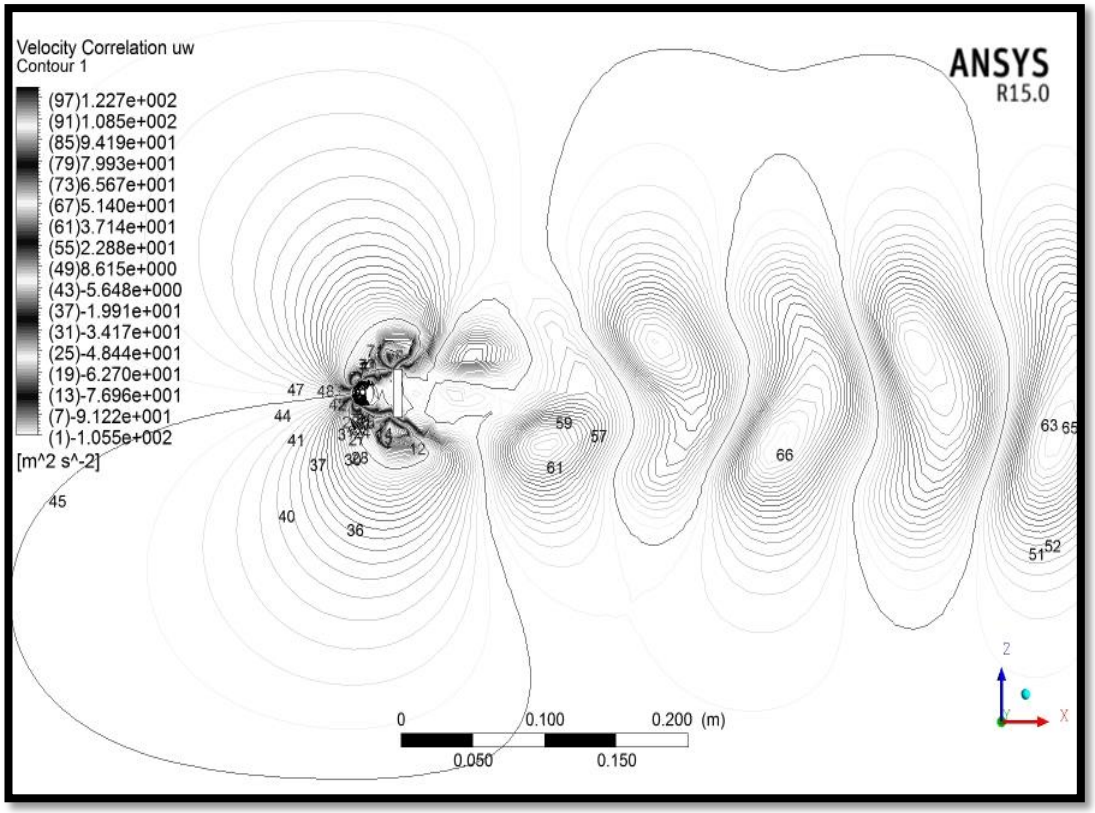

Figure 49. Contours *of* u' w' Velocity at t=0.200002s for $\frac{g}{w} = 0.8$

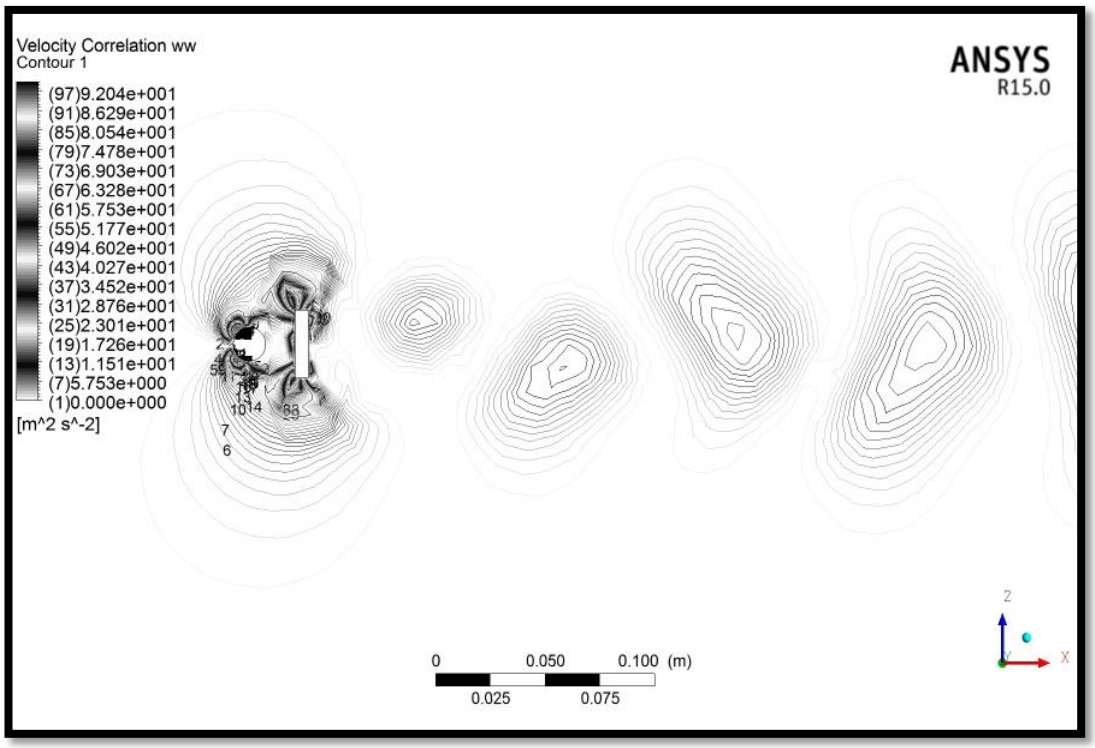

Figure 50. Contours of w' w' Velocity at t=0.200002s for $\frac{g}{w} = 0.8$

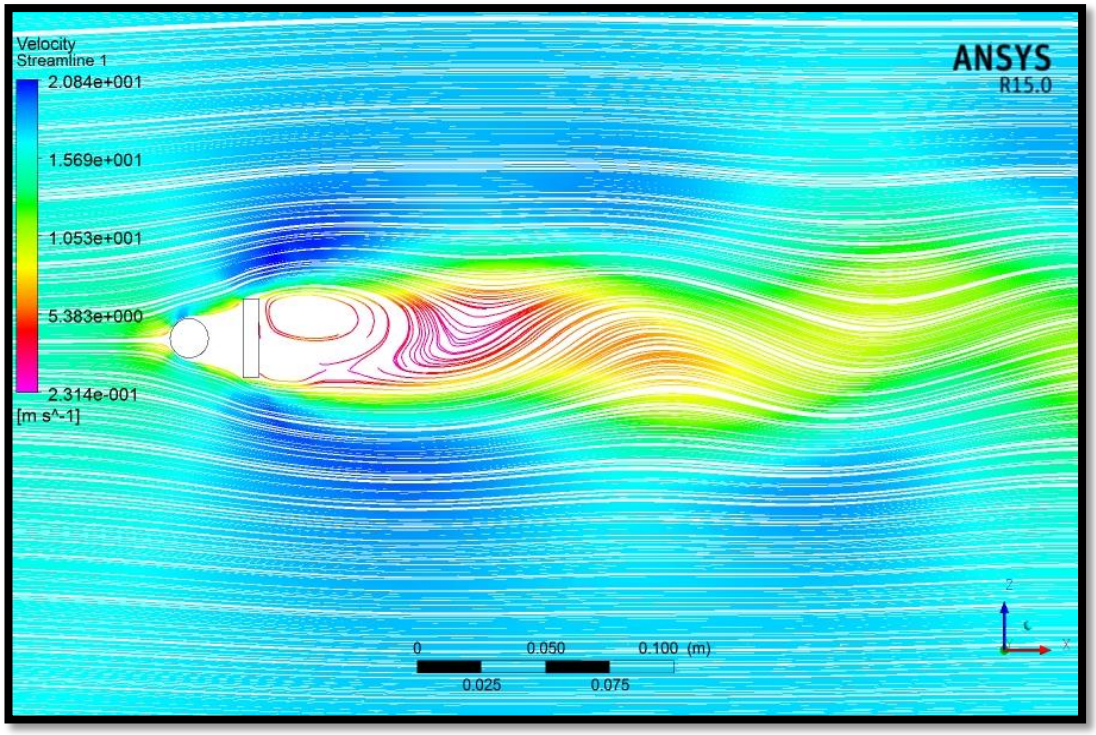

Figure 51. Velocity Streamlines at t=0.200002s for $\frac{g}{w} = 0.8$

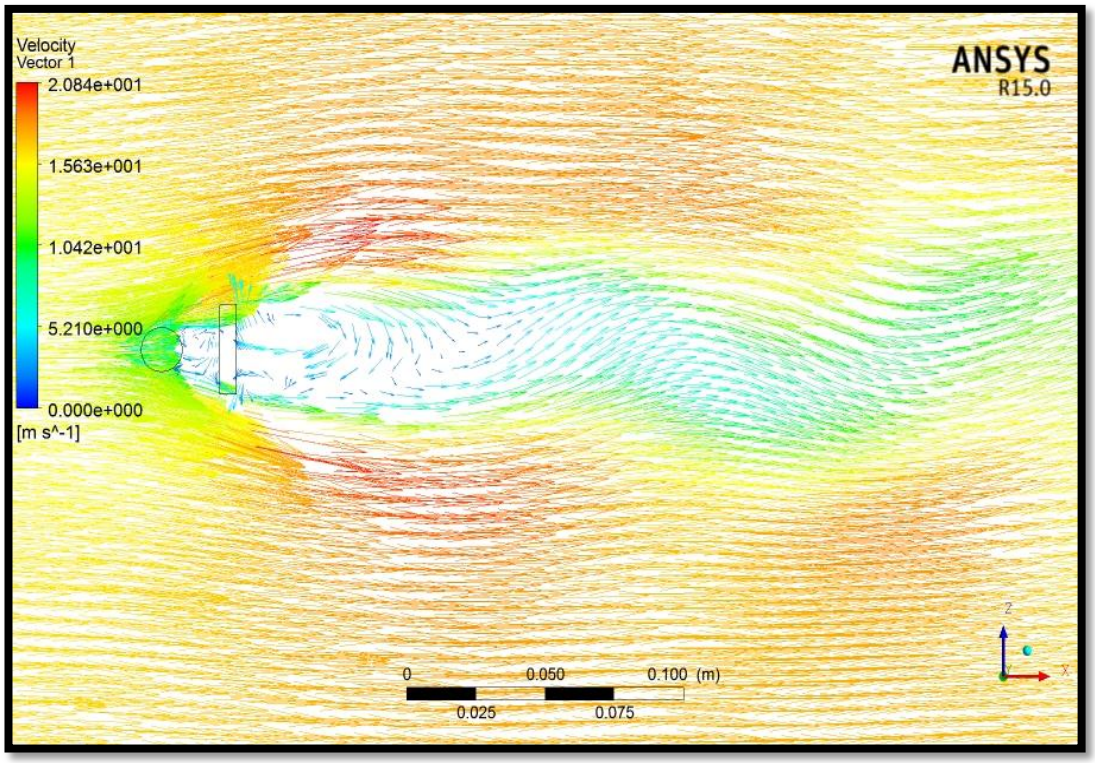

Figure 52. Velocity Vectors at t=0.200002s for $\frac{g}{w} = 0.8$

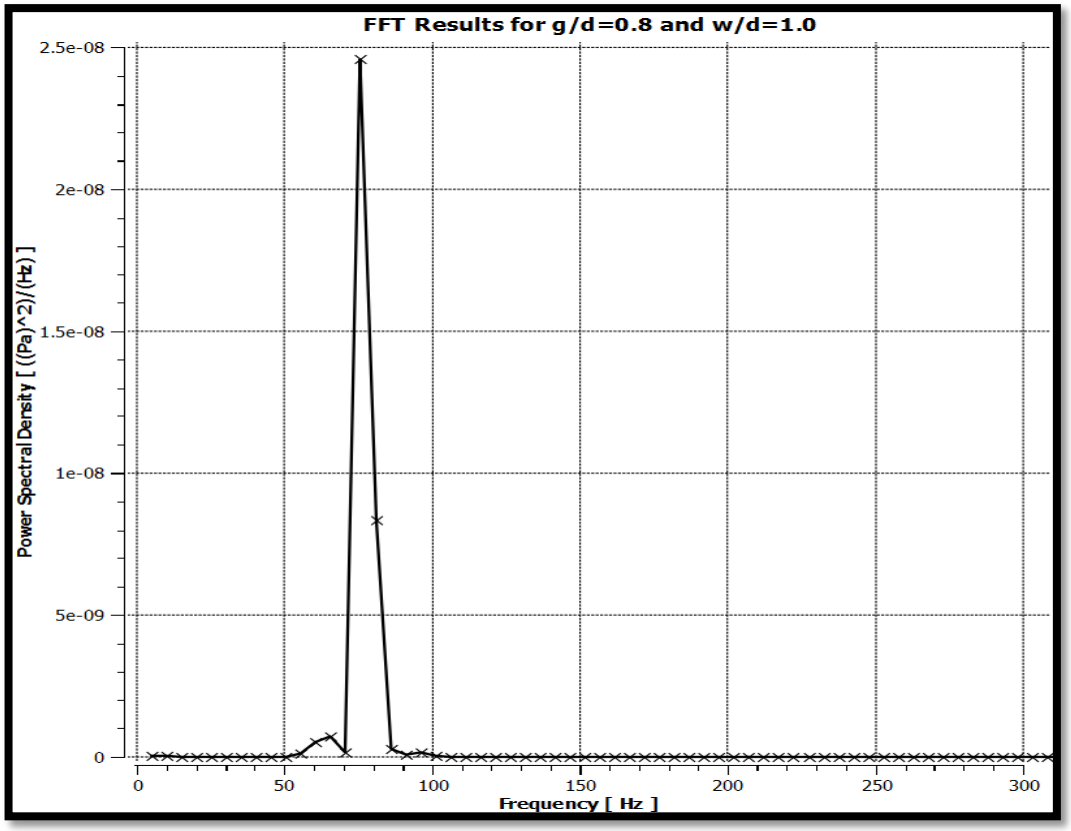

Figure 53. FFT Results for $\frac{g}{w} = 0.8$ and *w/d=2.0*

4.3 Summary of Results

Table 4.1 represent the change in shedding frequency and Strouhal number with respect to gap ratio and geometry for the same width and diameter plate and circular cylinder for both curve and FFT approaches.

Table 4.1 Calculated St and *f* for same width and diameter circular cylinder and plate

30 (*mm*) Cylinder and 30 (*mm*) Plate in Tandem				
	FFT		Using C_l Curve	
g/w	*f* (Hz)	St	*f* (Hz)	St
0.8	80.8080826	0.14781966	79.363731	0.1451776
0.867	80.8080826	0.14781966	78.1237	0.1429092
1	75.757576	0.13858093	75.7562959	0.1385786
2	70.7070694	0.1293422	69.443273	0.1270304
3	65.6565704	0.12010348	67.5664	0.1235971
4	64.9194565	0.1187551	64.93519	0.1187839

Table 4.2 illustrate the change of St Number and shedding frequency with respect to gap ratio for *w/d = 1.0*.

Table 4.2 Calculated St and *f* for *w/d = 1.0*

15 (*mm*) Cylinder and 30 (*mm*) Plate in Tandem				
	FFT		Using C_l Curve	
g/w	*f* (Hz)	St	*f* (Hz)	St
0.8	75.757576	0.13858093	76.9218	0.1407106
0.867	75.6660919	0.13841358	76.9218	0.1407106
1	74.6960144	0.13663905	73.5282	0.1345028
2	65.6565704	0.12010348	67.5664	0.1235971
3	65.5772781	0.11995844	66.6655	0.1219491
4	65.6565704	0.12010348	65.7884	0.1203446

Chapter 5

CONCLUSION

5.1 Summary

The effect of the turbulent wake of cylinder with two different diameters on the flat plates with the same width at several gap ratios was investigated using Computational Fluid Dynamics. The shedding period were used to obtain the frequency and Strouhal number for several cases.

For the same characteristic lengths of geometries, the shedding frequency and Strouhal number were in inverse proportion to the gap ratios. This fact was again true for circular cylinder with half diameter of the original one, i.e. again the shedding frequency and Strouhal number increased while the gap ratio decreased.

For each case with the same gap ratio, the Strohal number of the cases with the same plate width and cylinder diameter was higher than the cases with cylinder with 15 (*mm*) diameter, except for the case of gap ratio of 4.0. At this gap ratio the shedding frequency and St Number of the case with 15 (*mm*) cylinder were higher than the case of 30 (*mm*) cylinder.

5.2 Future Studies

According to the results of this study, there is a critical gap ratio presence which the behavior of the shedding phenomena changes by exceeding this gap ratio for different geometries. Very high simulation time and powerful computer is needed to

calculate this critical ratio. The study of the nature of this singular phenomena is recommended for future studies.

REFERENCES

[1] Versteeg H. K., Malalasekera W. (2007). *An introduction to computational fluid dynamics: the finite volume method*. Second Edition. New Jersey: Prentice Hall, pp 300-305.

[2] Bearman P.W. (1965). *Investigation of the flow behind a two-dimensional model with a blunt trailing edge and fitted with splitter plates.* Journal of Fluid Mechanics, Volume 21, pp 241-255.

[3] Auteri F., Belan M., Gibertini G., Grassi D. (2008). *Normal flat plates in tandem: An experimental investigation.* Journal of Wind Engineering and Industrial Aerodynamics, Volume 96 (6-7), pp 872-879.

[4] Liu C. H., Chen J. M. (2002). *Observations of hysteresis in flow around two square cylinders in a tandem arrangement*. Journal of Wind Engineering and Industrial Aerodynamics, Volume 90 (9), pp 1019-1050.

[5] Yen S.C., San K.C., Chuang T.H. (2008). *Interactions of tandem Square cylinders at low Reynolds numbers*. Experimental Thermal and Fluid Science, Volume 32 (4), pp 927-938.

[6] Xu, G., Zhou, Y. (2004). *Strouhal numbers in the wake of two inline cylinders.* Experiments in Fluids, Volume 37, pp 248-256.

[7] Wei C.Y., Chang J.R. (2002). *Wake and base-bleed flow downstream of bluff bodies with different geometry*. Experimental Thermal and Fluid Science, Volume 26 (1), pp 39-52

[8] Mazharoglu C., Hacisevki H. (1999). *Coherent and incoherent flow structures behind a normal flat plate*. Experimental Thermal and Fluid Science, Volume 19(3), pp 160-167.

[9] Hacisevki, H., Mazharoglu, C. (2000). *Triple decomposition technique applied for near wake flow measurement*. Experimental Thermal and Fluid Science, Volume19(3), pp 272-275.

[10] Kiya, M., Matsumara, M. (1988). *Incoherent turbulence structure in the near wake of a normal plate.* Journal of Fluid Mechanics, Volume 190, pp 343-356.

[11] Auteri F., Belan M., Gibertini G., Grassi D. (2008). *Normal flat plates in tandem: An experimental investigation.* Journal of Wind Engineering and Industrial Aerodynamics, Volume 96 (6-7), pp 872-879.

[12] Martinuzzi RJ., Havel B. (2004). *Vortex shedding from two surface-mounted cubes in tandem*. International Journal of Heat and Fluid Flow, Volume 25, pp 364–372

[13] Bosch, G., Rodi, W. (1996). *Simulation of vortex shedding past a square cylinder near a wall.* International Journal of Heat and Fluid Flow, Volume 17(3), pp 267-275.

[14] Kato, M., Launder, B. E. (1993). *The modeling of turbulent flow around stationary and vibrating square cylinders*. Proc. 9th Symposium on Turbulent Shear Flows, Kyoto, Japan, 10-4

[15] Edamoto, K., Kawahara, M. (1998). *Finite element analysis of two and three-dimensional flows around square columns in tandem arrangement.* International Journal for Numerical Methods in Fluids, Volume 28, pp 95–112.

[16] Wu, J., Hu, Y. (1995). *A numerical study of wake interference behind two side-by-side and tandem circular cylinders*. Journal of the Chinese Society of Mechanical Engineers, Volume 16 (2), pp 109-122.

[17] Cengel, A., CIMBALA, M. (2006). *Fluid mechanics fundamentals and applications*. New York: McGraw-Hill, pp 570

[18] Holmes J. D. (2001). *Wind loading of structures*. First Edition. London: Spon Press, pp 157-158.

[19] Menter, F. R. (1993), *Zonal Two Equation k-ω Turbulence Models for Aerodynamic Flows*, AIAA Journal, Volume. 32(7), pp 93-98.

[20] Menter, F. R. (1994), *Two-Equation Eddy-Viscosity Turbulence Models for Engineering Applications*, AIAA Journal, Volume. 32(8), pp. 1598-1605.